

Electronic Supplementary Information (ESI)

**Molecular Structure Controlled Self-Assembly of Pyridine Appended Fluorophores:  
Multi-stimuli Fluorescence responses and Fabricating Rewritable/Self-Erasable  
Fluorescent Platforms**

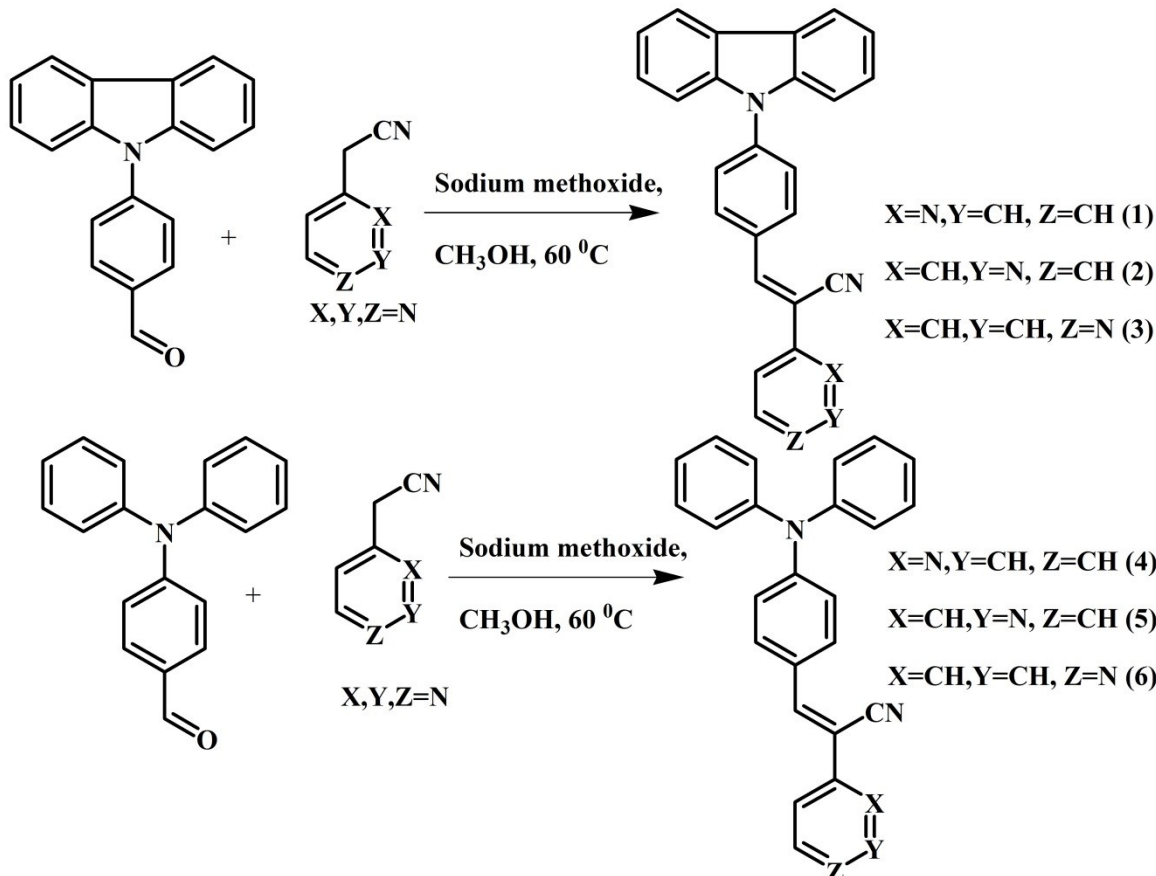
Parthasarathy Gayathri,<sup>[a]</sup> Mehboobali Pannipara,<sup>[b,c]</sup> Abdullah G. Al-Sehemi,<sup>[b,c]</sup> Dohyun Moon<sup>\*[d]</sup> Savarimuthu Philip Anthony<sup>\*[a]</sup>

<sup>a)</sup>School of Chemical & Biotechnology, SASTRA Deemed University, Thanjavur-613401, Tamil Nadu, India. Fax: +914362264120; Tel: +914362264101; E-mail: philip@biotech.sastra.edu

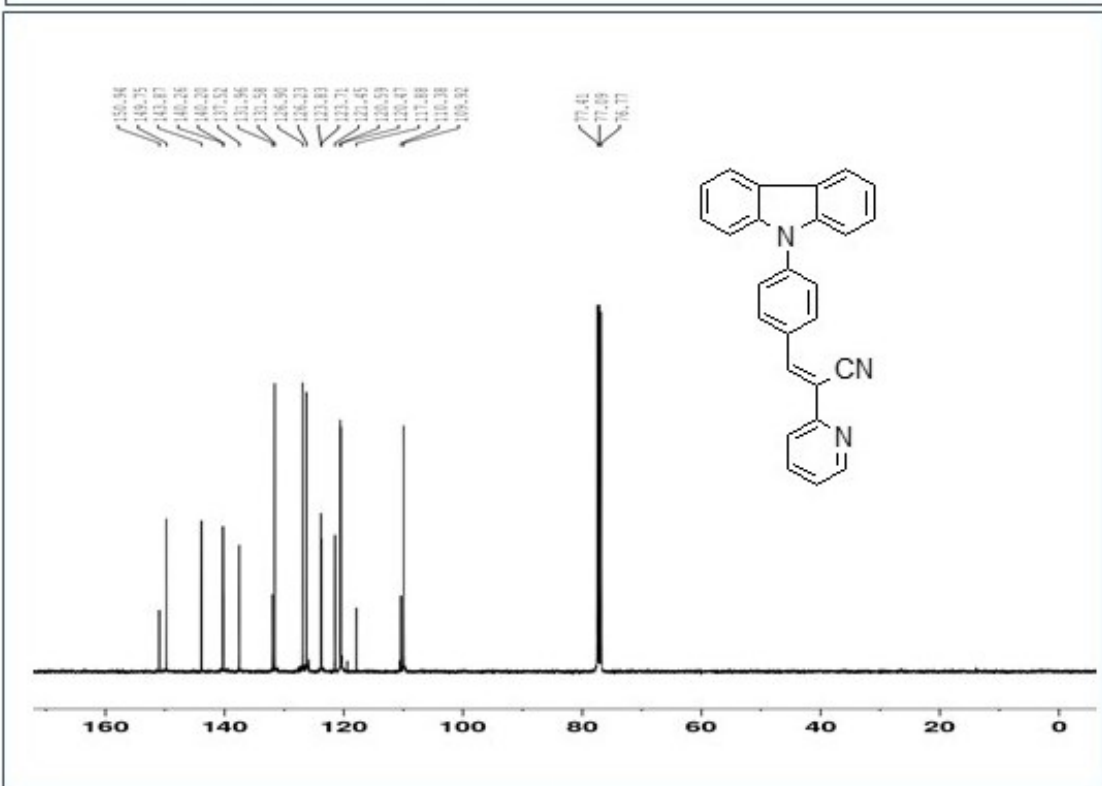
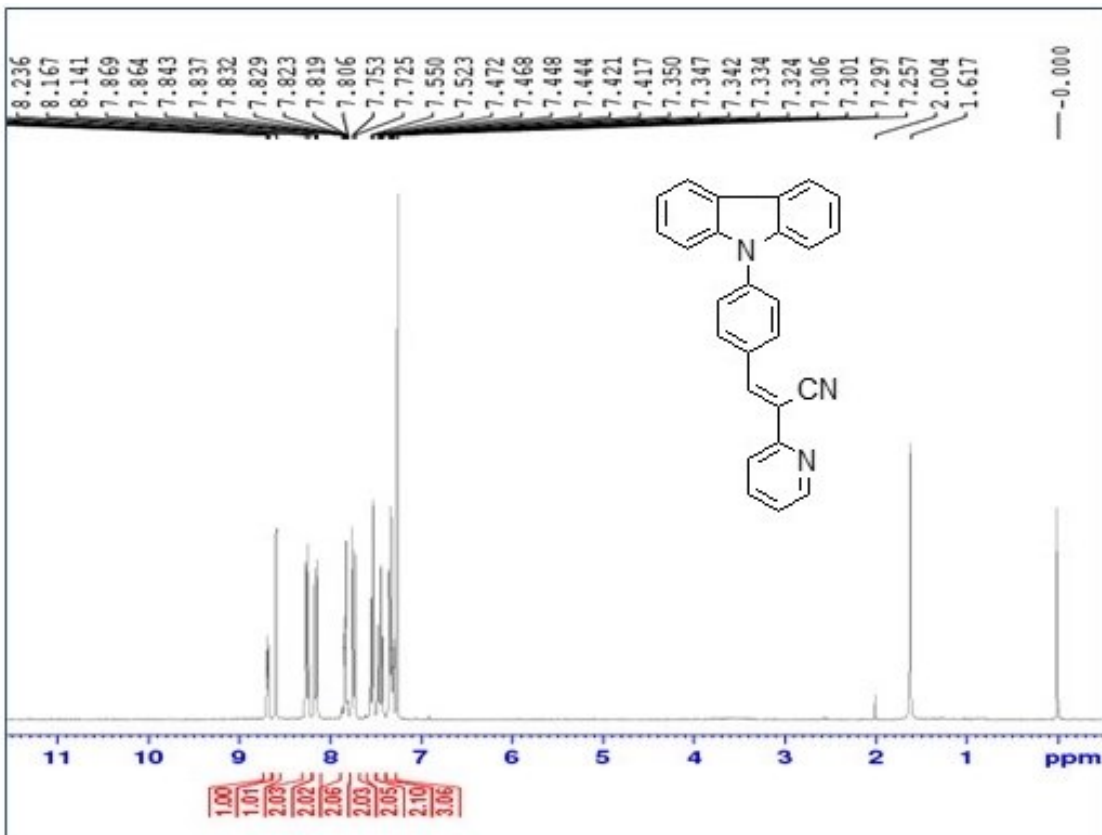
<sup>b)</sup>Department of chemistry, King Khalid University, Abha 61413, Saudi Arabia.

<sup>c)</sup>Research center for Advanced Materials Science, King Khalid University, Abha 61413, Saudi Arabia.

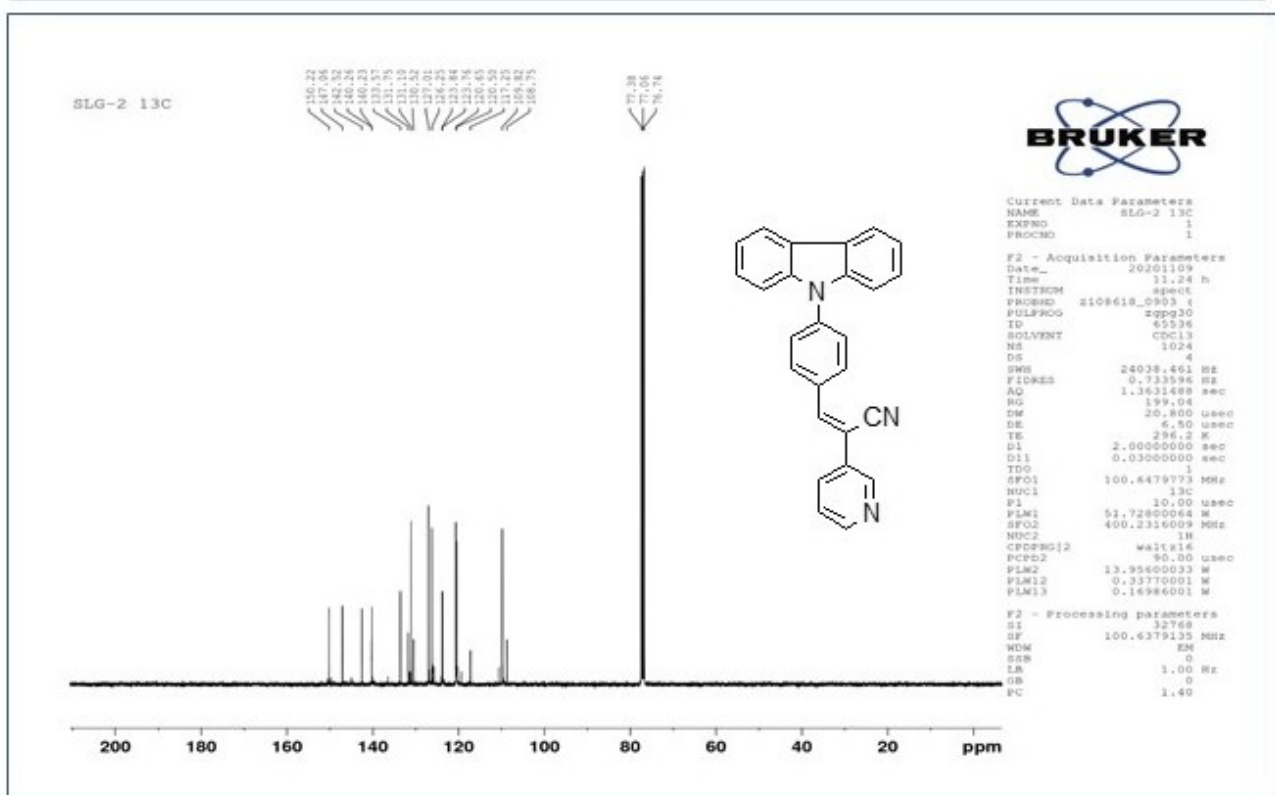
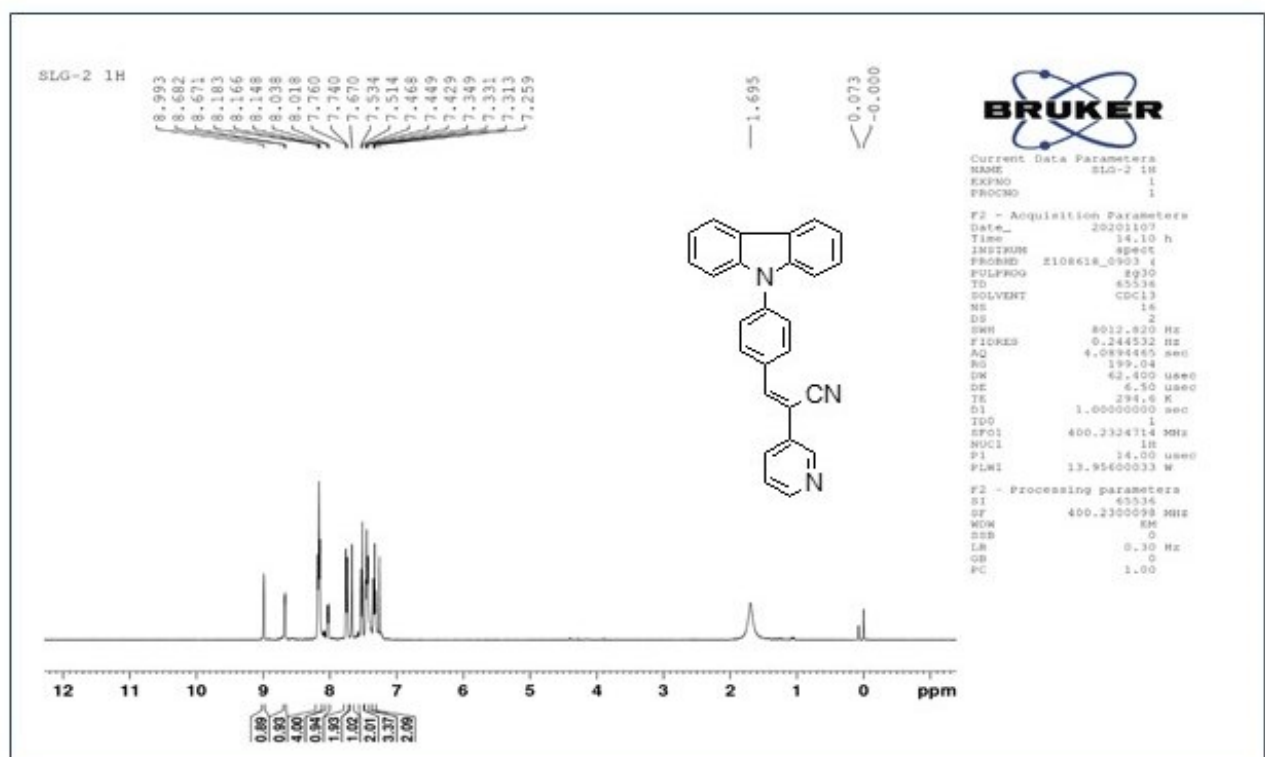
<sup>b)</sup>Beamline Department, Pohang Accelerator Laboratory, 80 Jigokro-127beongil, Nam-gu, Pohang, Gyeongbuk, Korea, Email: dmoon@postech.ac.kr



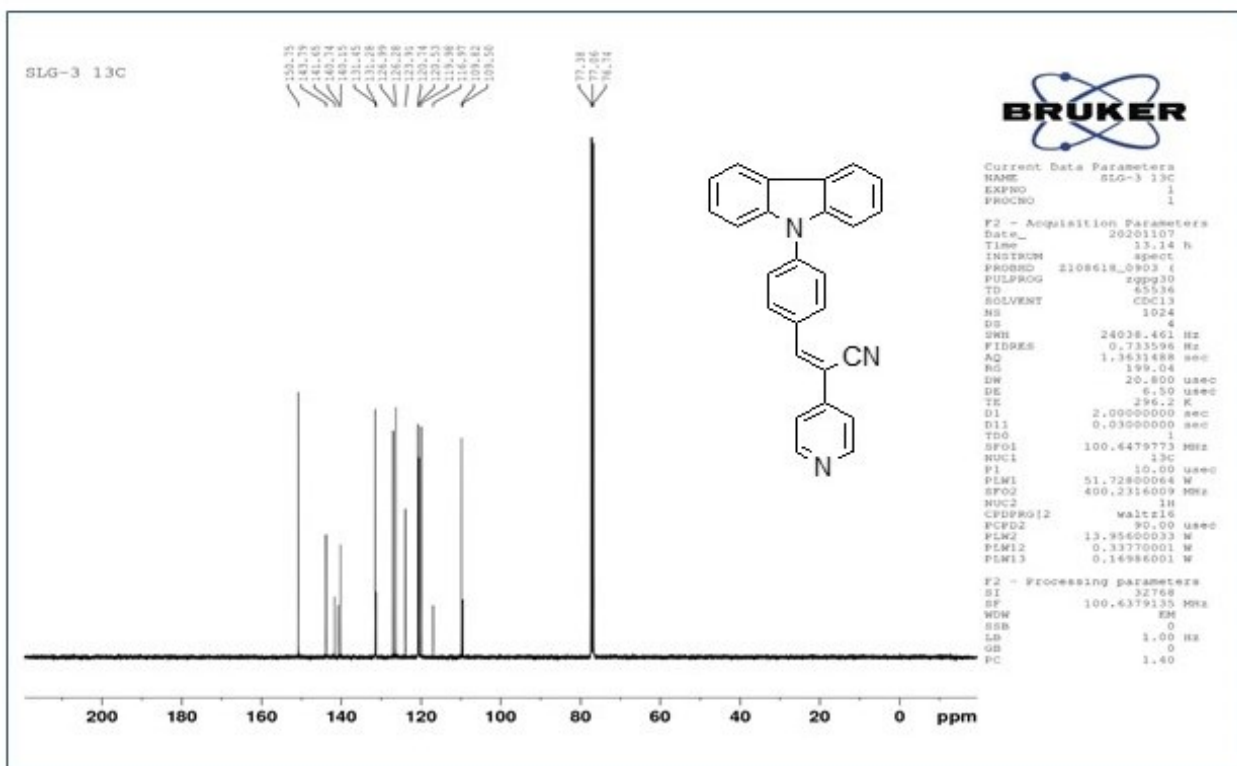
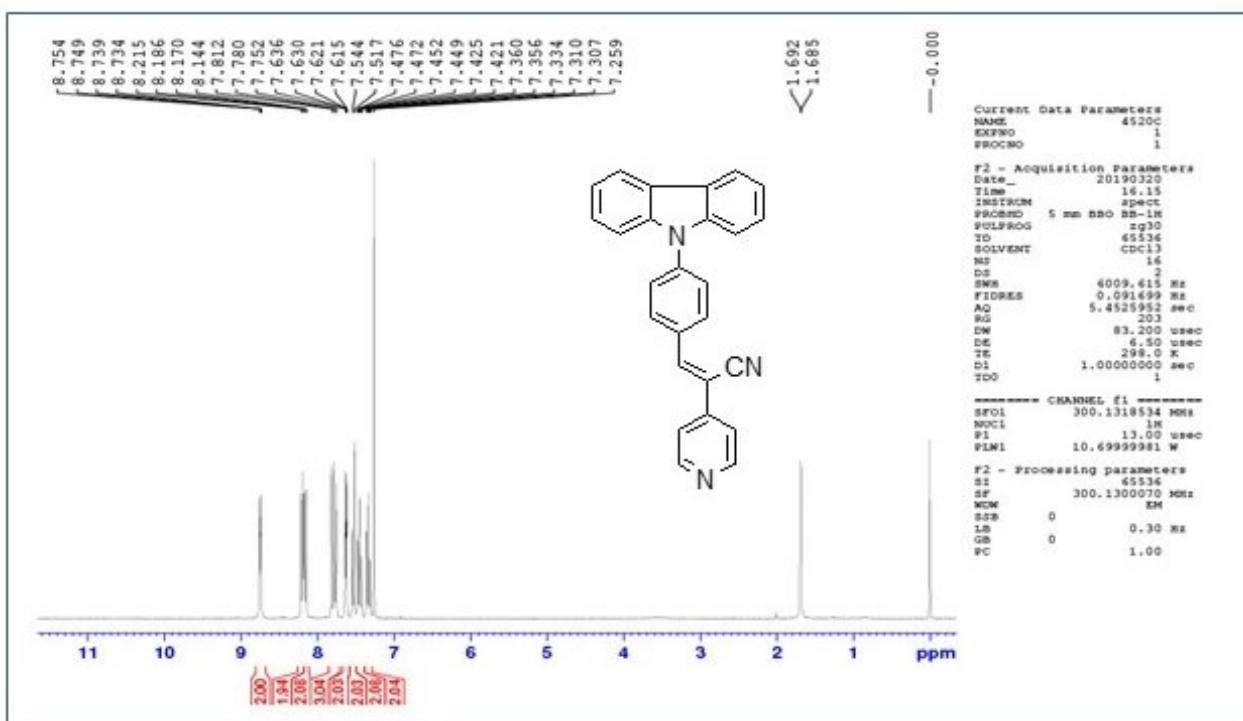
Scheme S1. Synthesis of carbazole and triphenylamine based isomers (1-6).



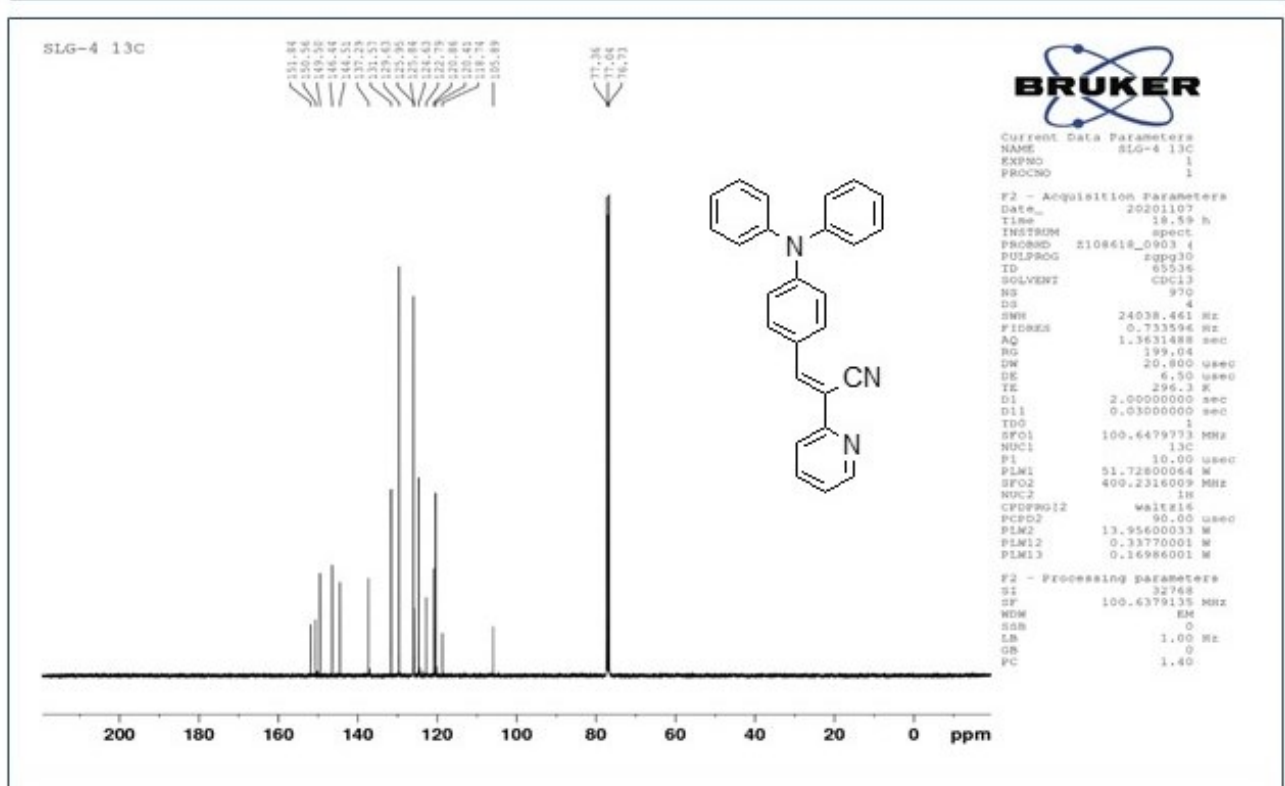
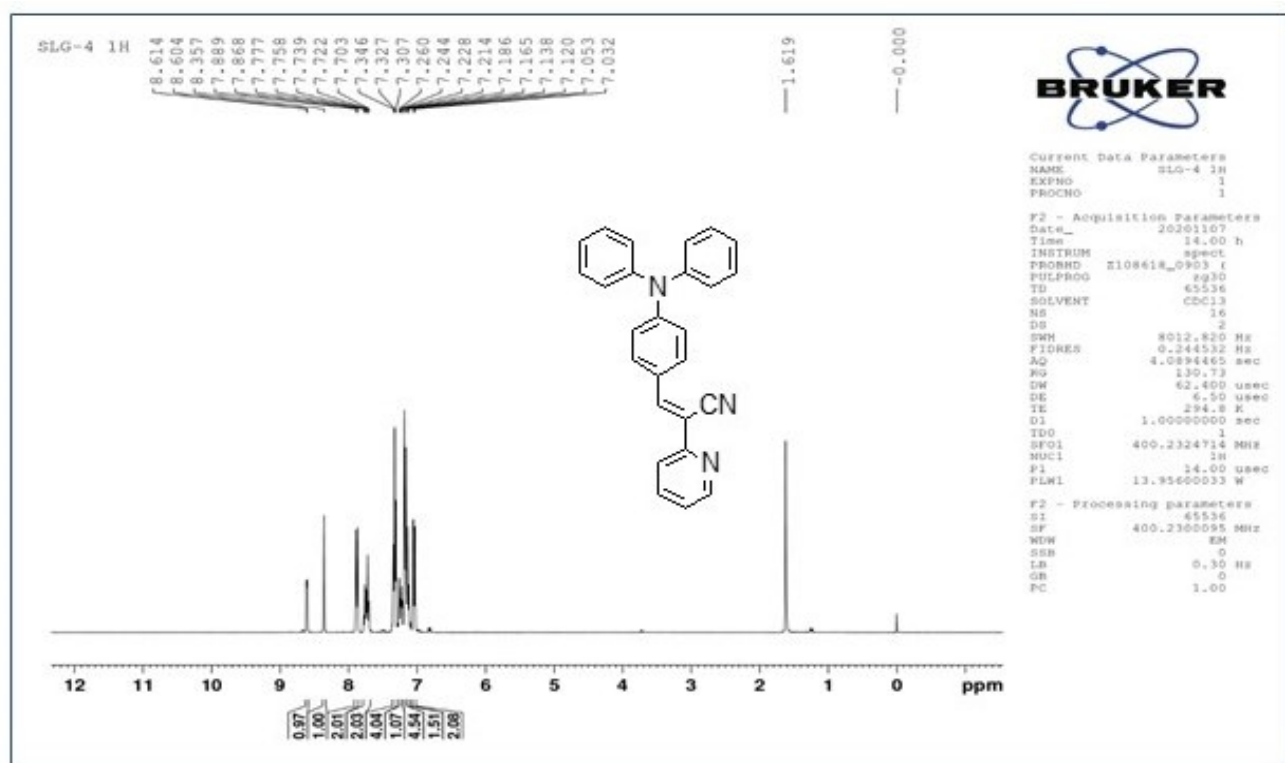
*<sup>1</sup>H* and *<sup>13</sup>C* NMR of **I**.



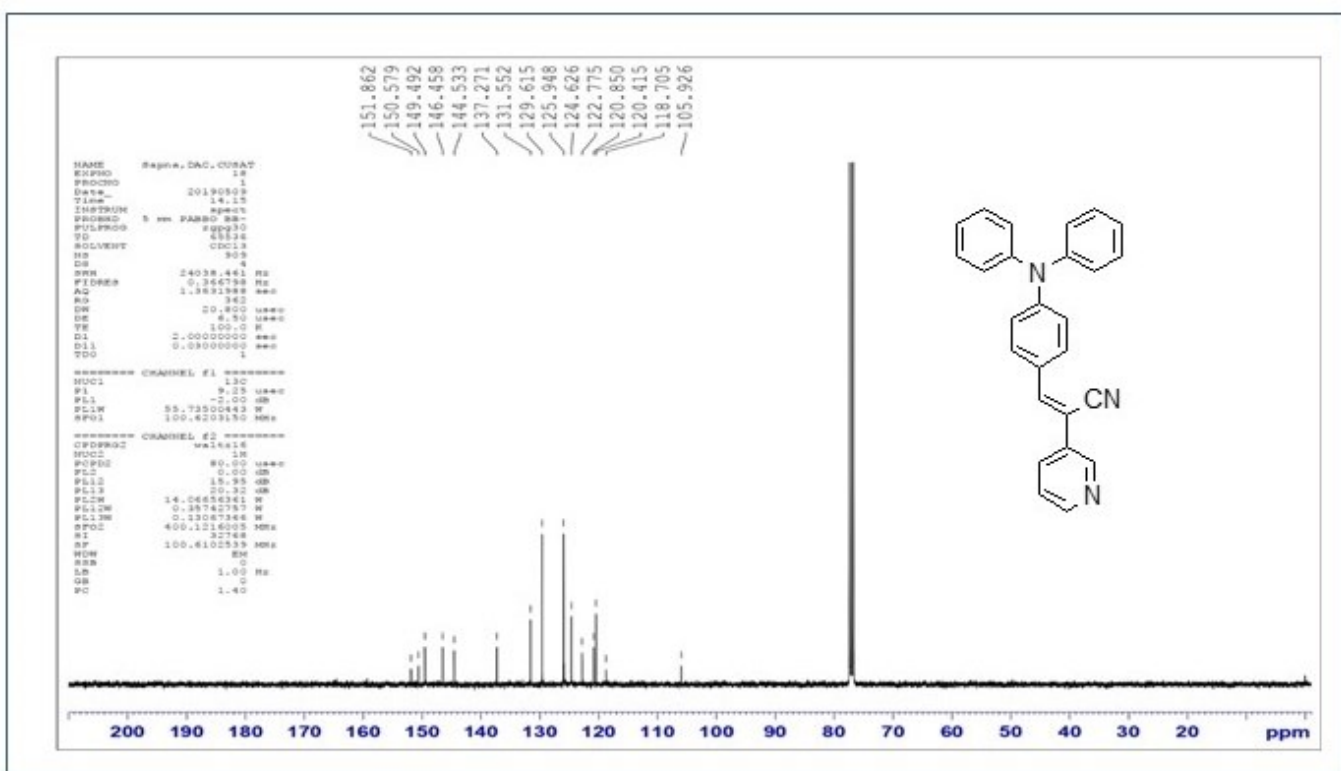
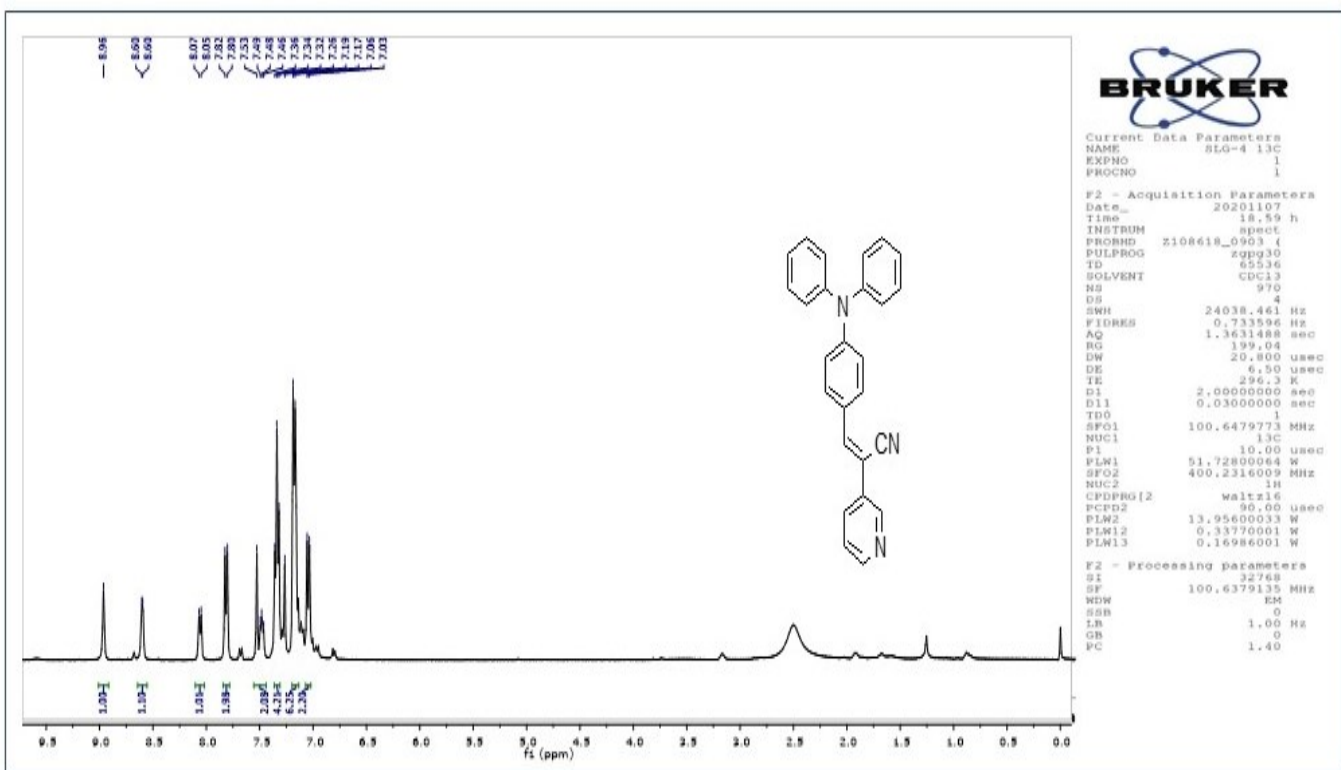
$^1H$  and  $^{13}C$  NMR of **2**.



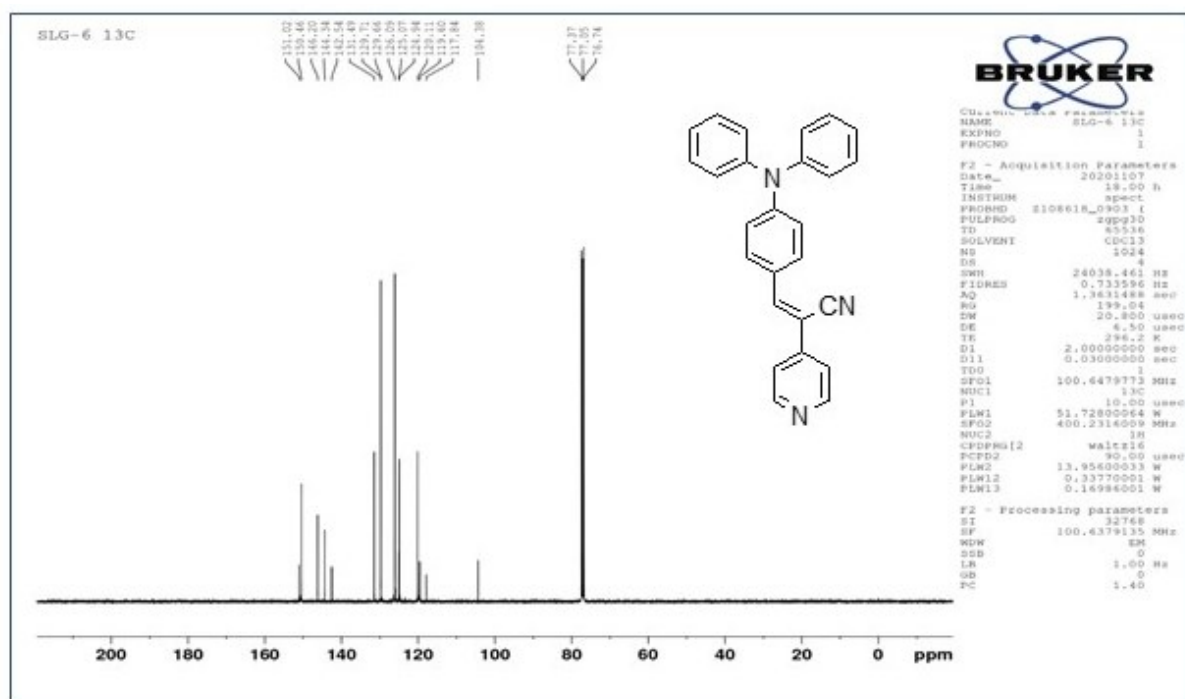
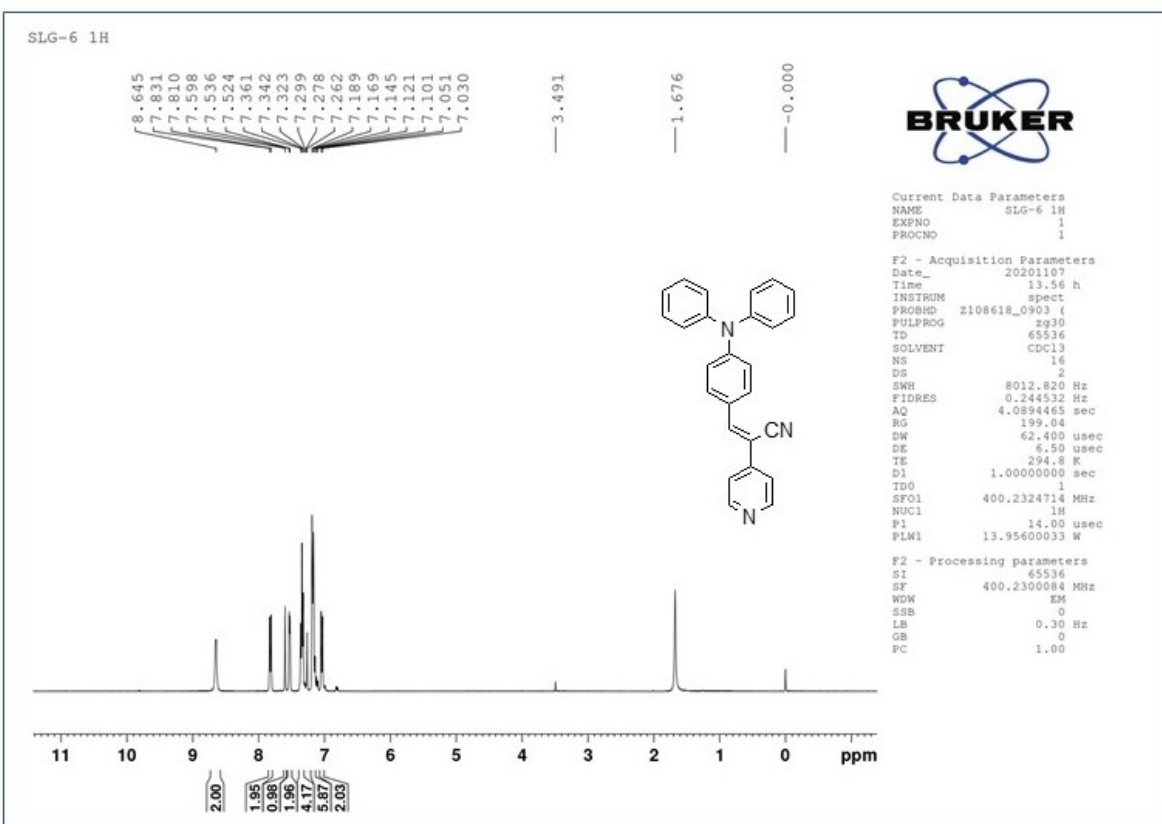
$^1H$  and  $^{13}C$  NMR of **3**.



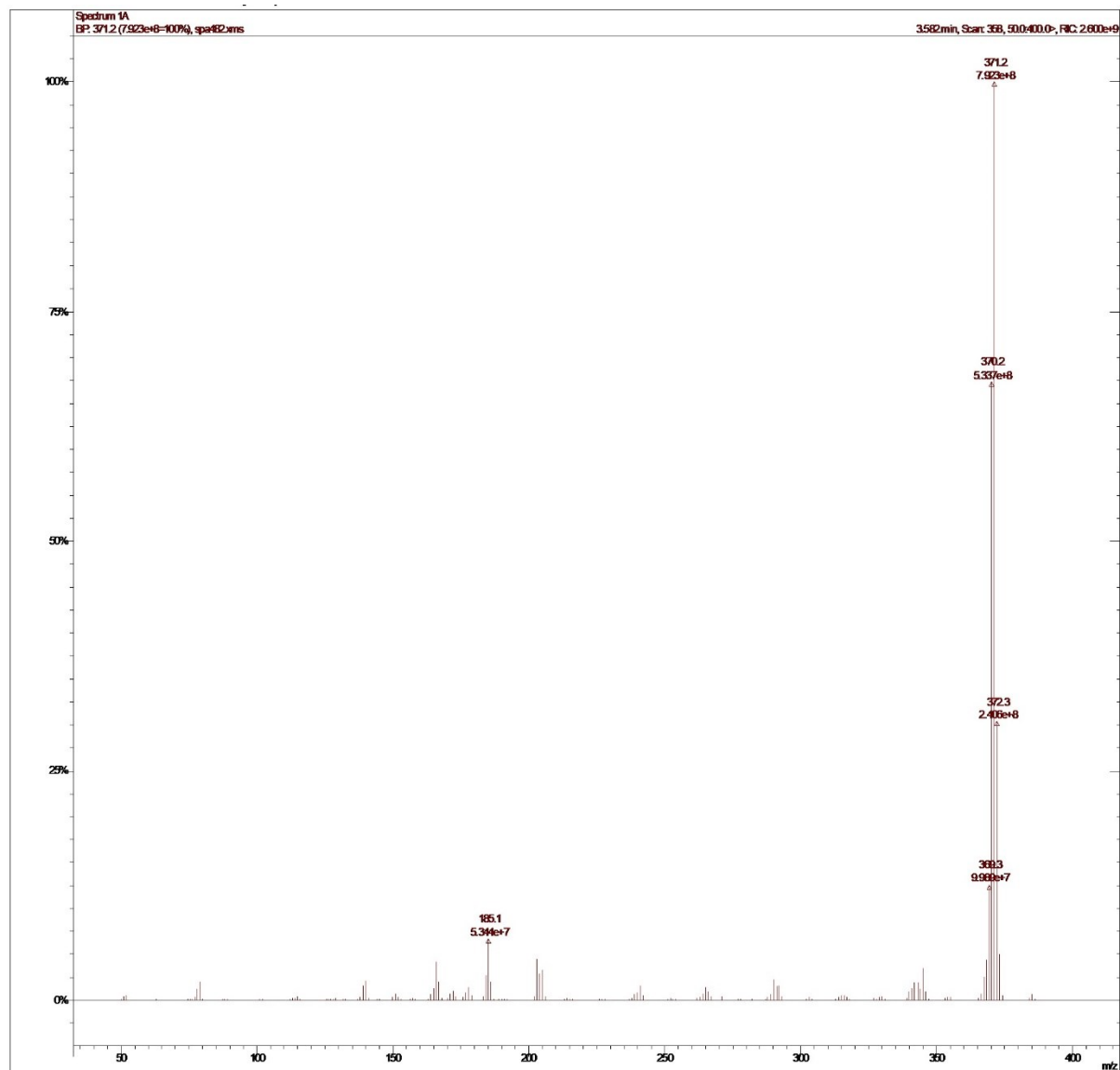
$^1H$  and  $^{13}C$  NMR of **4**.



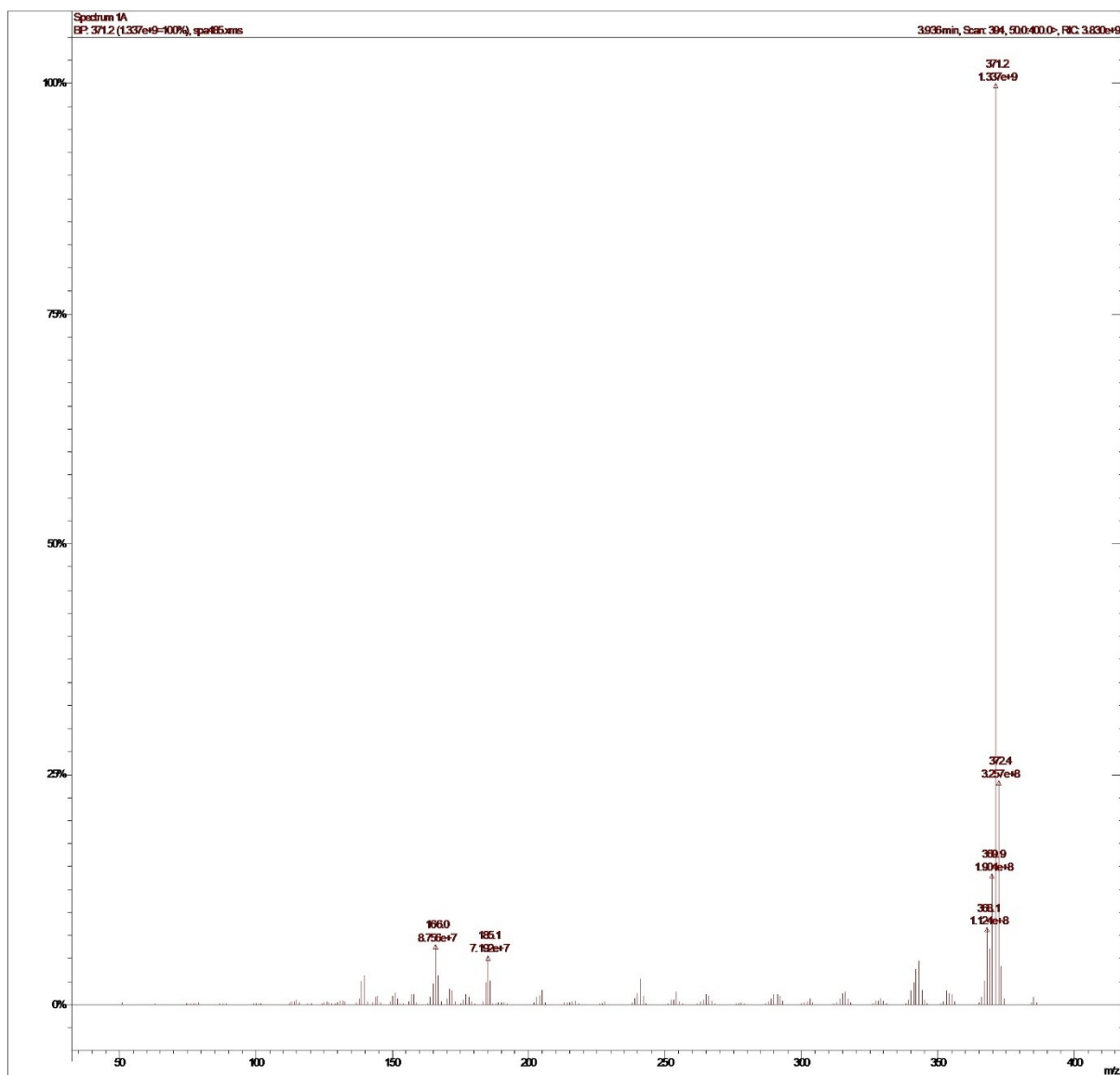
$^1H$  and  $^{13}C$  NMR of **5**.



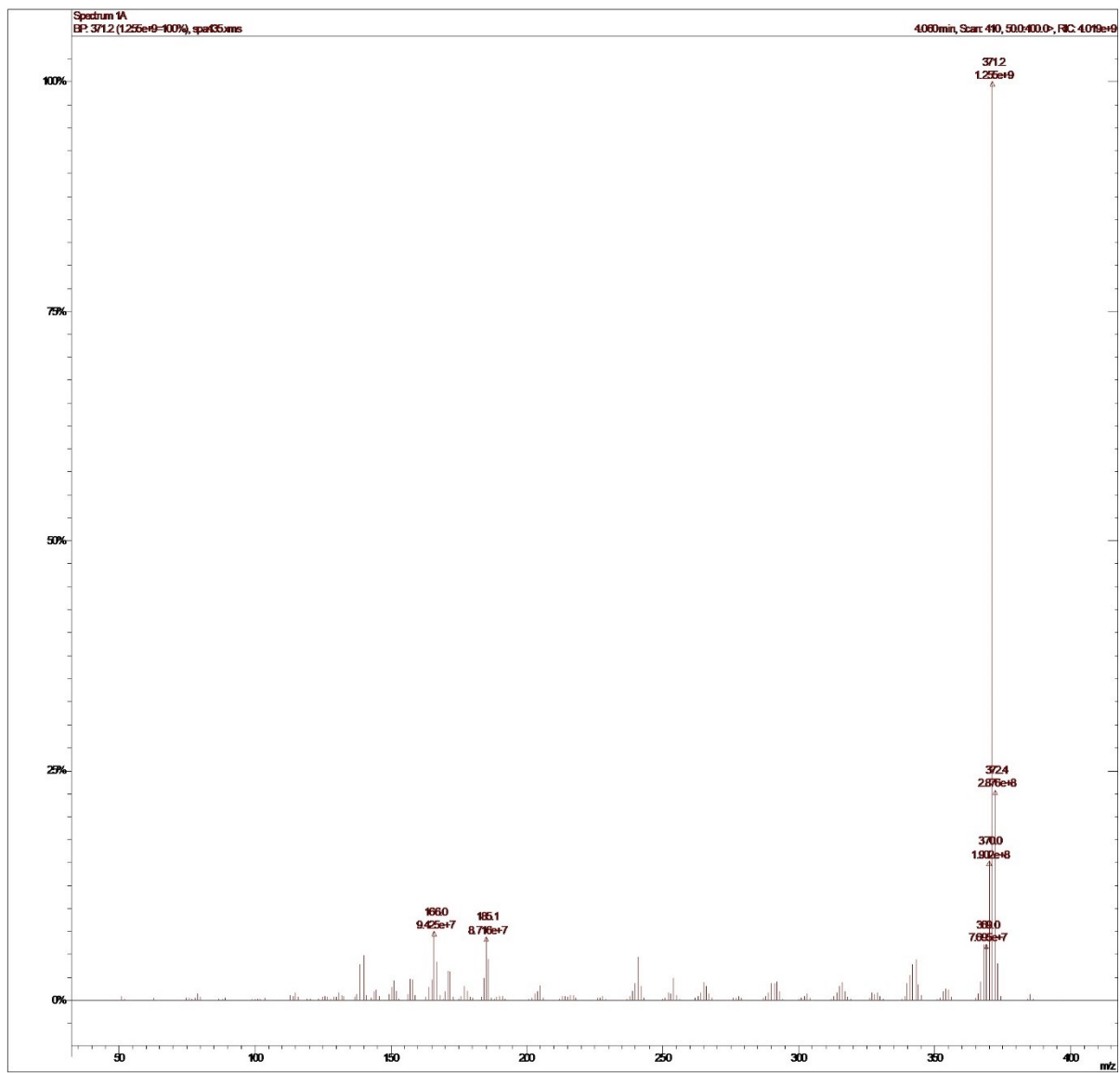
$^1H$  and  $^{13}C$  NMR of **6**.



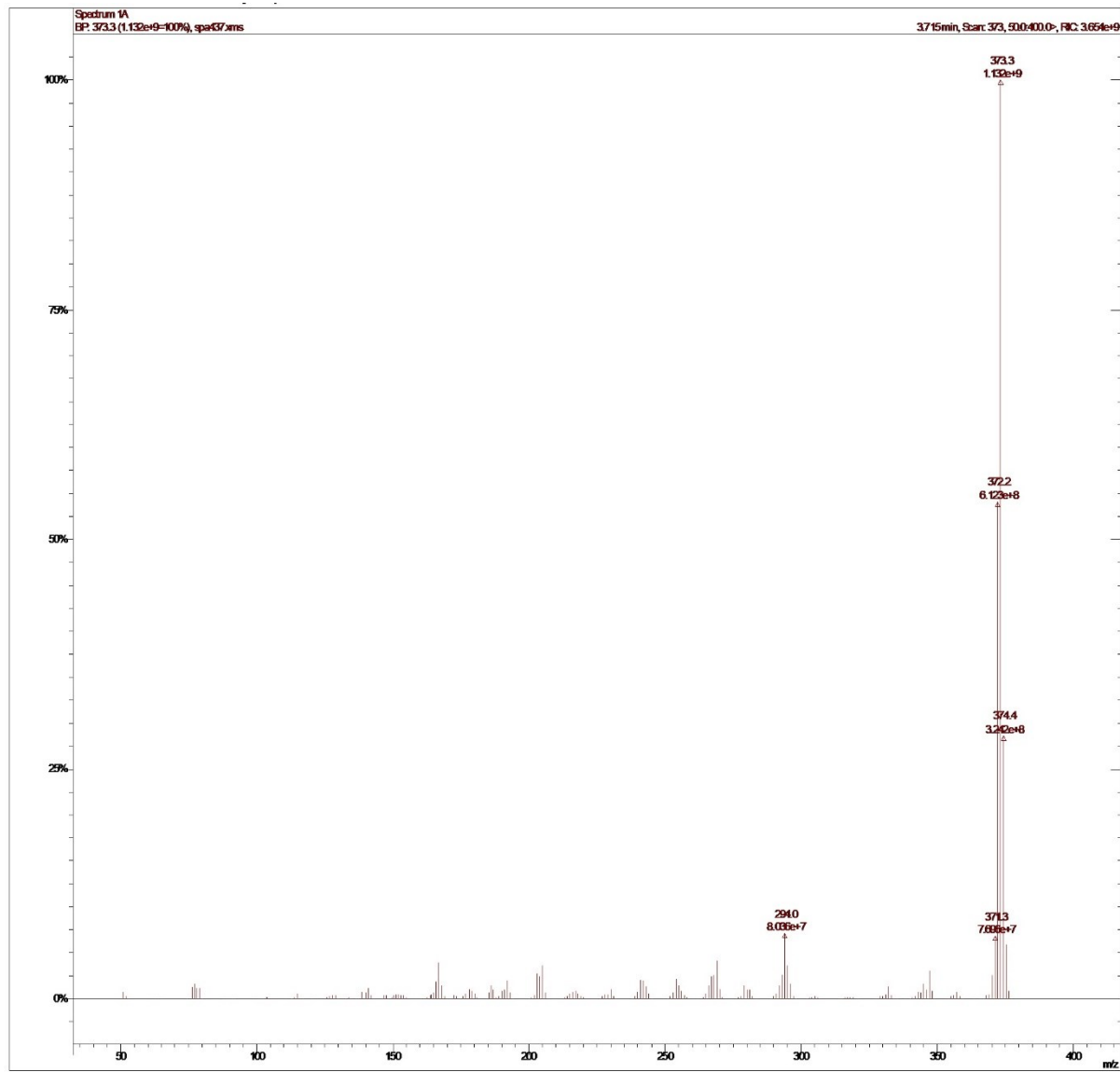
**1:** m/z calculated for  $C_{26}H_{17}N_3$  ( $M + H$ ): 371.14, found: 371.2



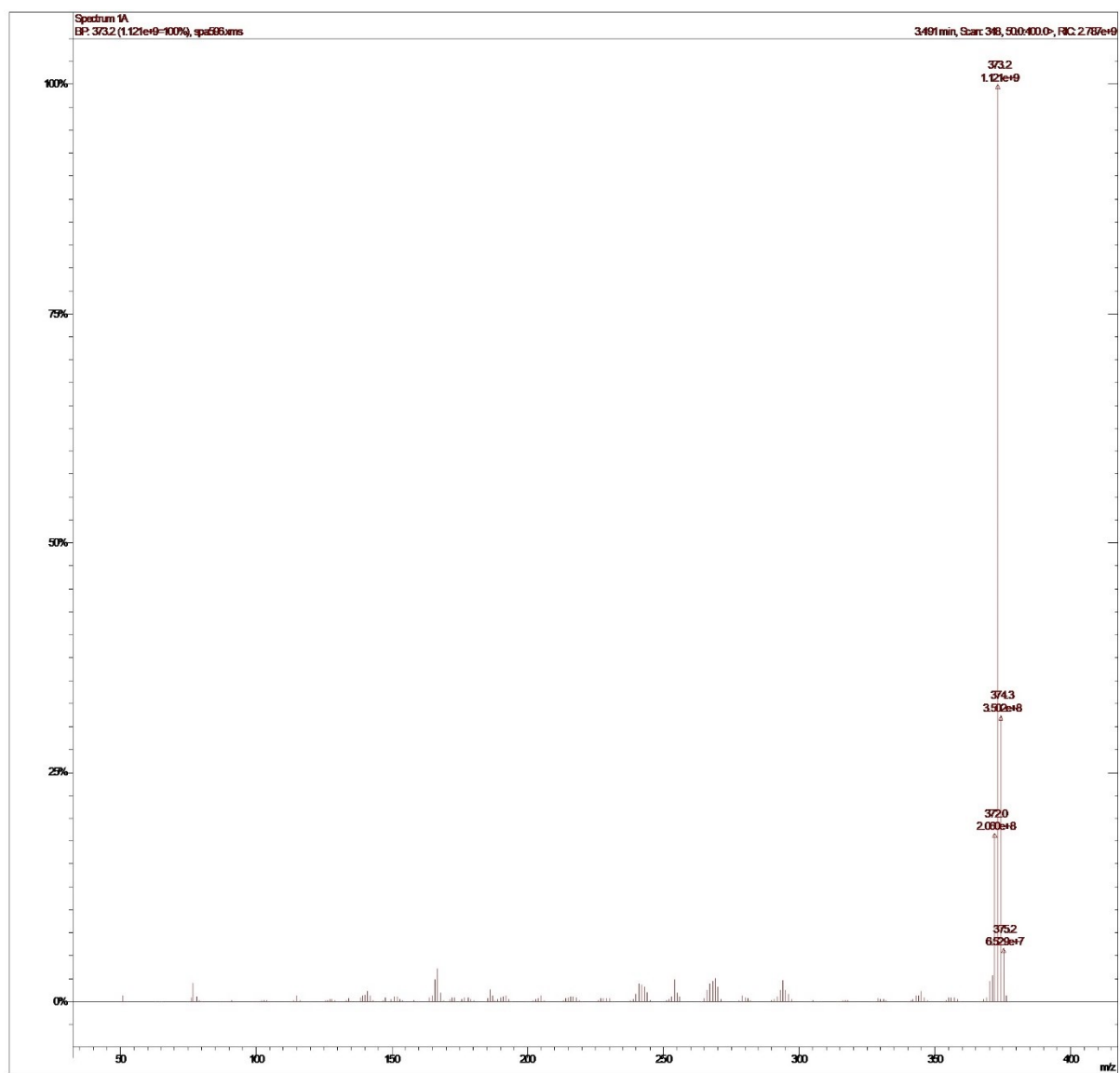
**2:**  $m/z$  calculated for  $C_{26}H_{17}N_3 (M + H)$ : 371.14, found: 371.2



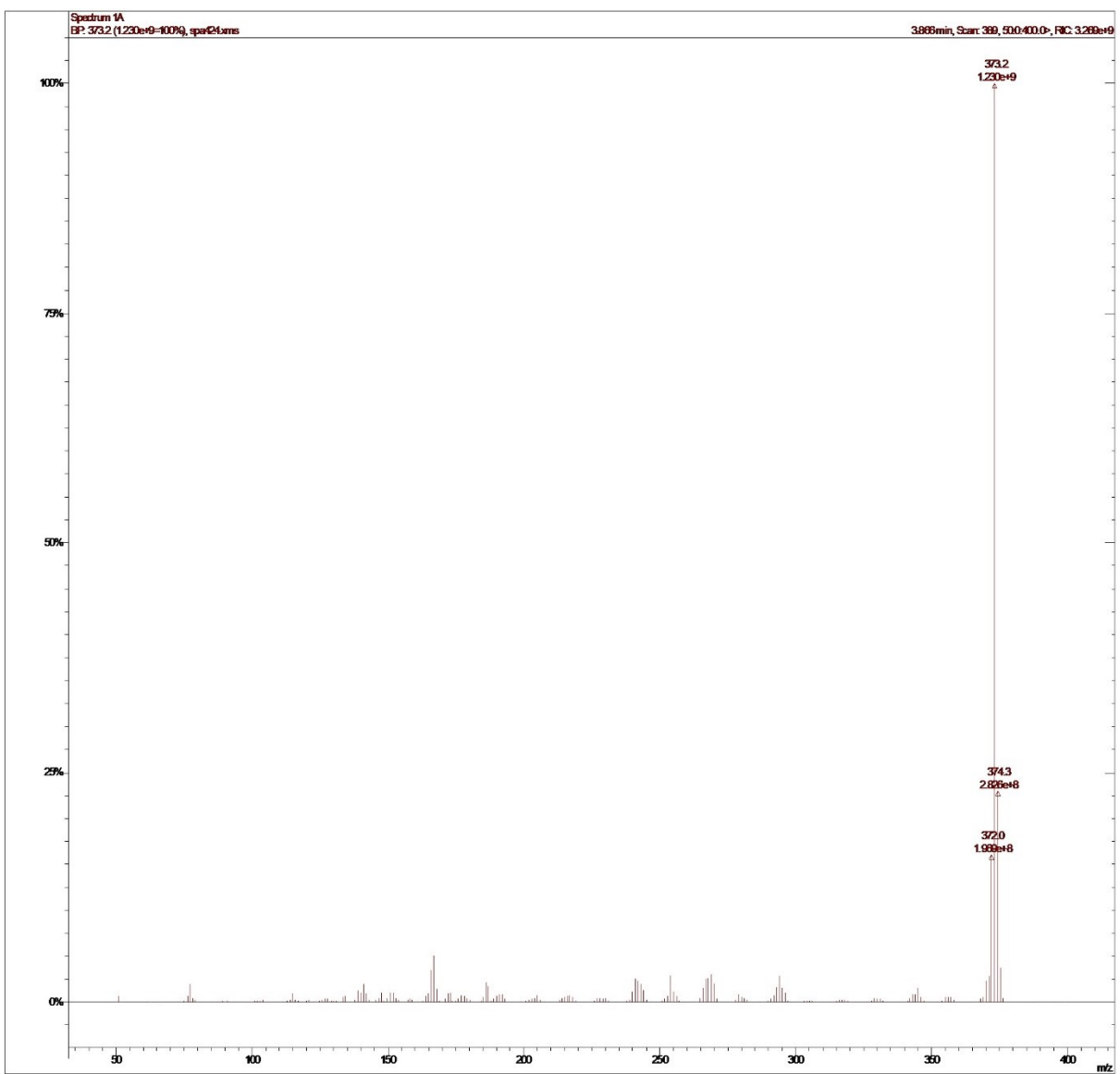
3: m/z calculated for  $C_{26}H_{17}N_3$  ( $M + H$ ): 371.14, found: 371.2



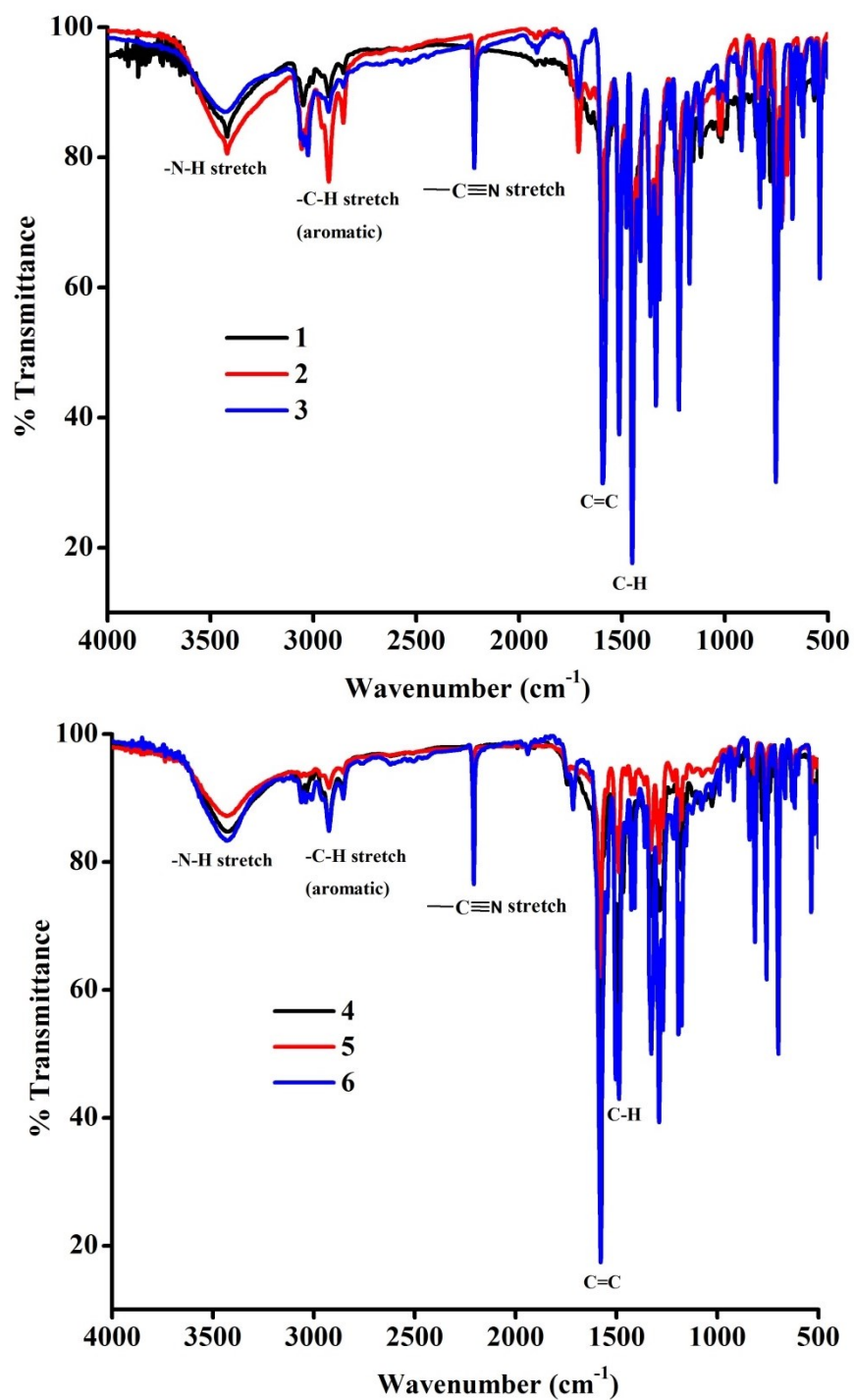
4:  $m/z$  calculated for  $C_{26}H_{19}N_3 (M + H)$ : 373.16, found: 373.3



5: m/z calculated for  $C_{26}H_{19}N_3$  ( $M + H$ ): 373.16, found: 373.2



**6:** m/z calculated for  $C_{26}H_{19}N_3$  ( $M + H$ ): 373.16, found: 373.2



IR spectra of **1-6**.

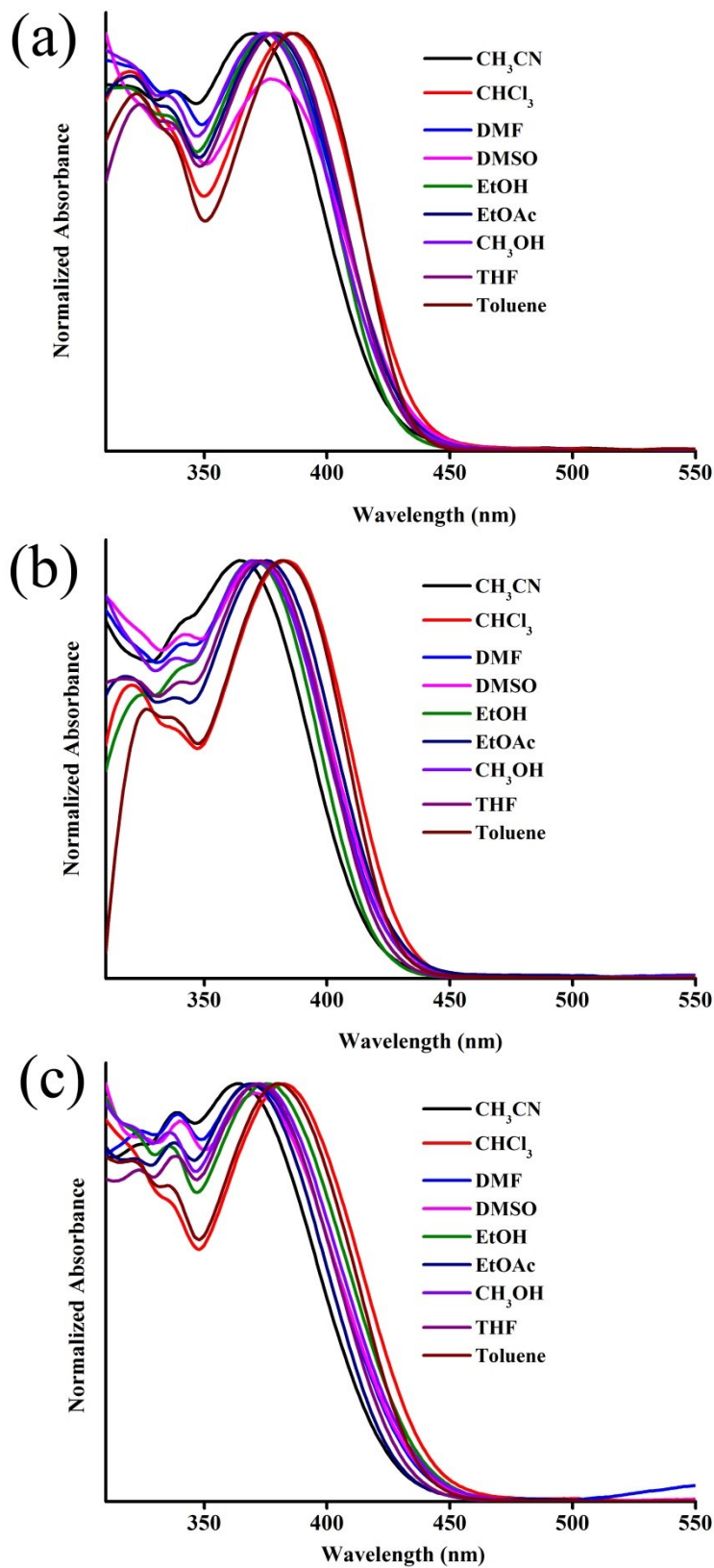


Fig. S1. Absorption spectra of (a) **1**, (b) **2** and (c) **3** in different solvents ( $10^{-4}$  M).

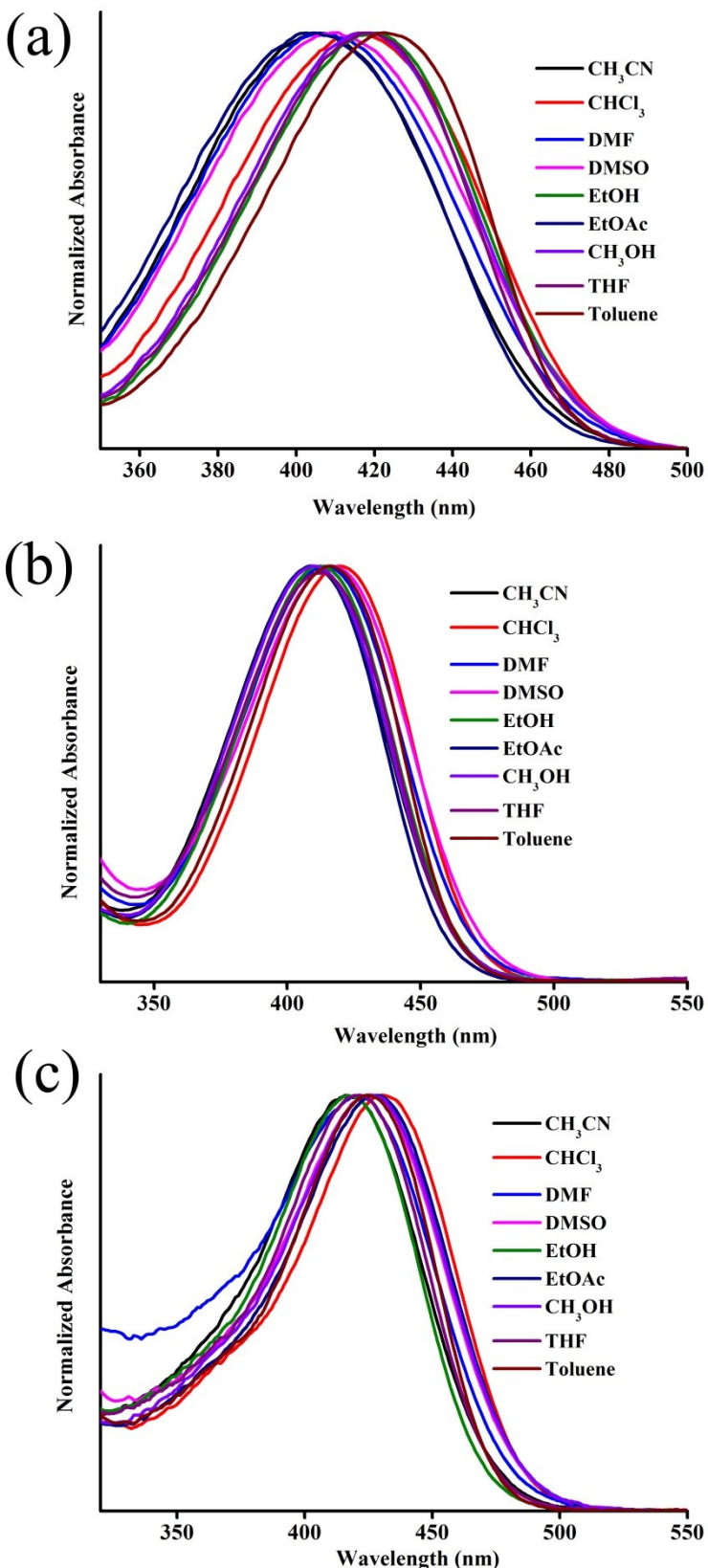


Fig. S2. Absorption spectra of (a) **4**, (b) **5** and (c) **6** in different solvents ( $10^{-4}$  M).

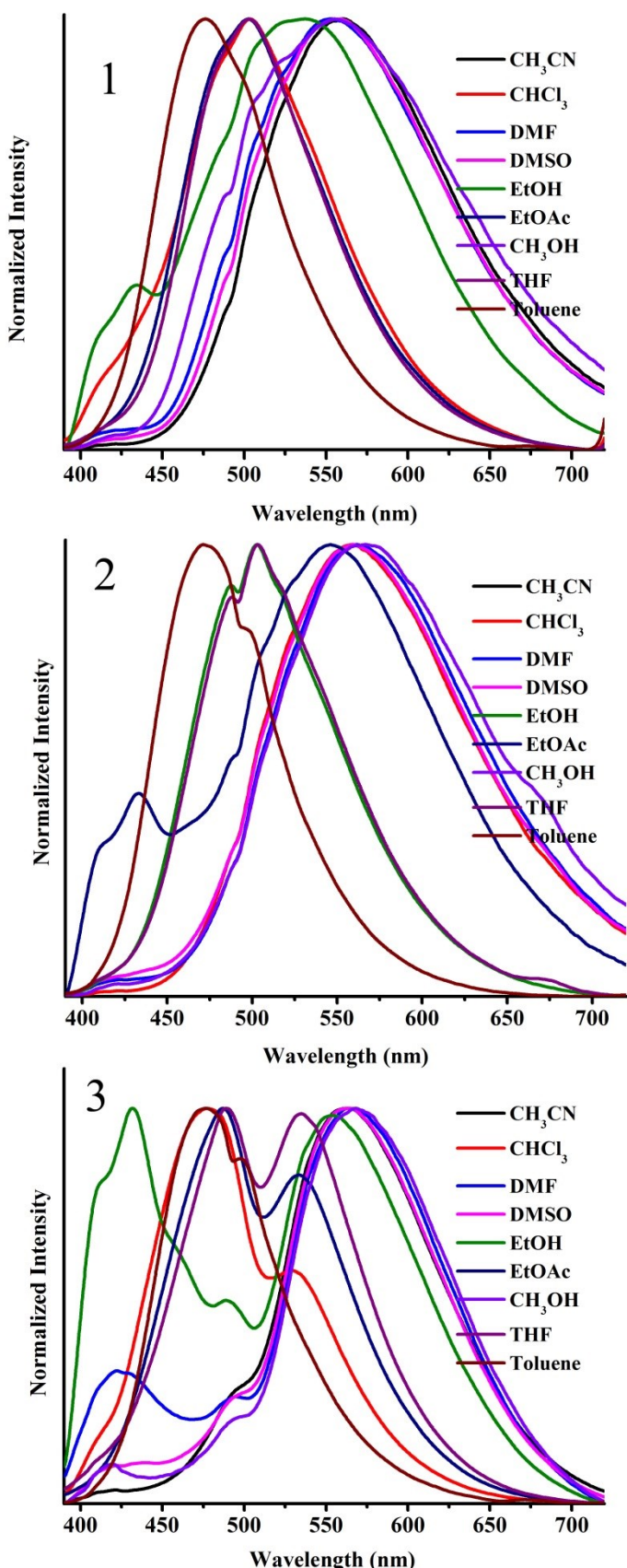


Fig. S3. Fluorescence spectra of **1-3** in different solvents ( $10^{-4}$  M).

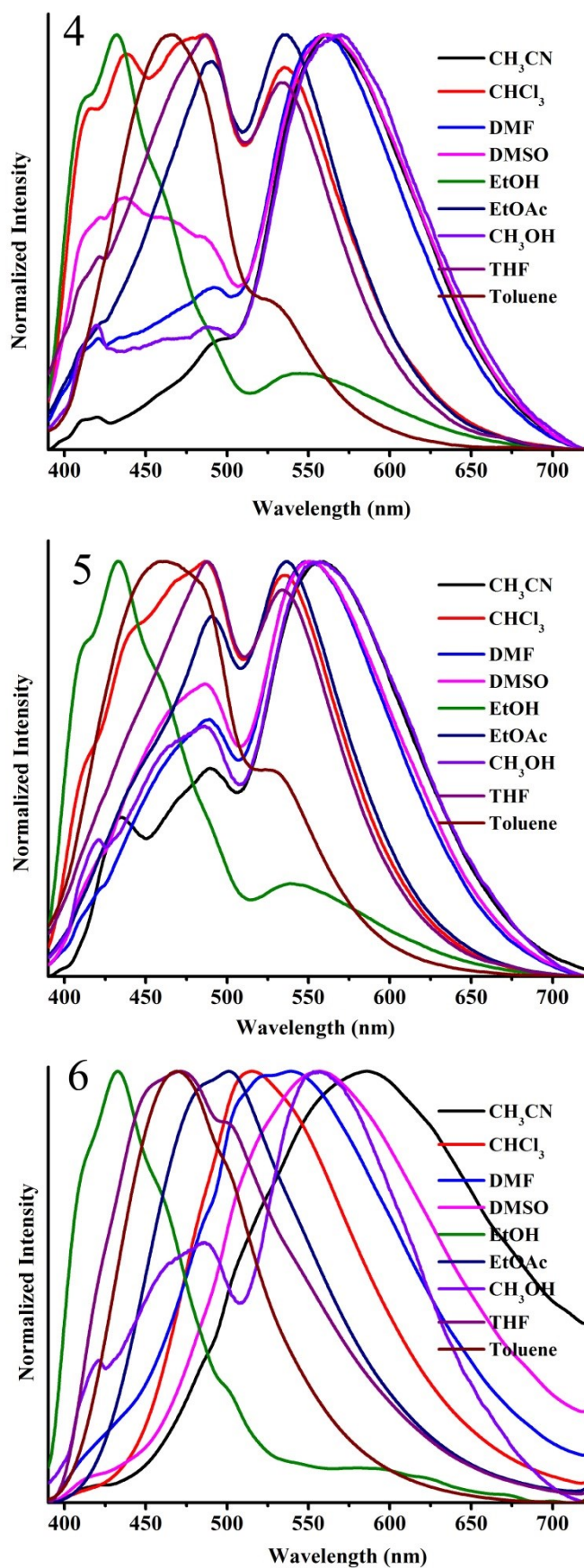


Fig. S4. Fluorescence spectra of **4-6** in different solvents ( $10^{-4}$  M).

Table S1. Fluorescence efficiency of **1-6** compared to quinine sulfate in different solvent polarity.

Solvents	Quantum Yield ( $\Phi_f$ )					
	<b>1</b>	<b>2</b>	<b>3</b>	<b>4</b>	<b>5</b>	<b>6</b>
CH <sub>3</sub> CN	0.02	0.01	0.034	0.007	0.010	0.03
CHCl <sub>3</sub>	0.23	0.15	0.27	0.74	0.62	0.34
DMF	0.06	0.12	0.15	0.21	0.32	0.1
DMSO	0.07	0.06	0.07	0.19	0.21	0.12
Ethyl acetate	0.081	0.19	0.23	0.20	0.23	0.29
Ethanol	0.05	0.05	0.07	0.08	0.09	0.09
Methanol	0.001	0.05	0.02	0.04	0.03	0.01
THF	0.11	0.08	0.15	0.28	0.37	0.31
Toluene	0.15	0.19	0.23	0.30	0.51	0.48

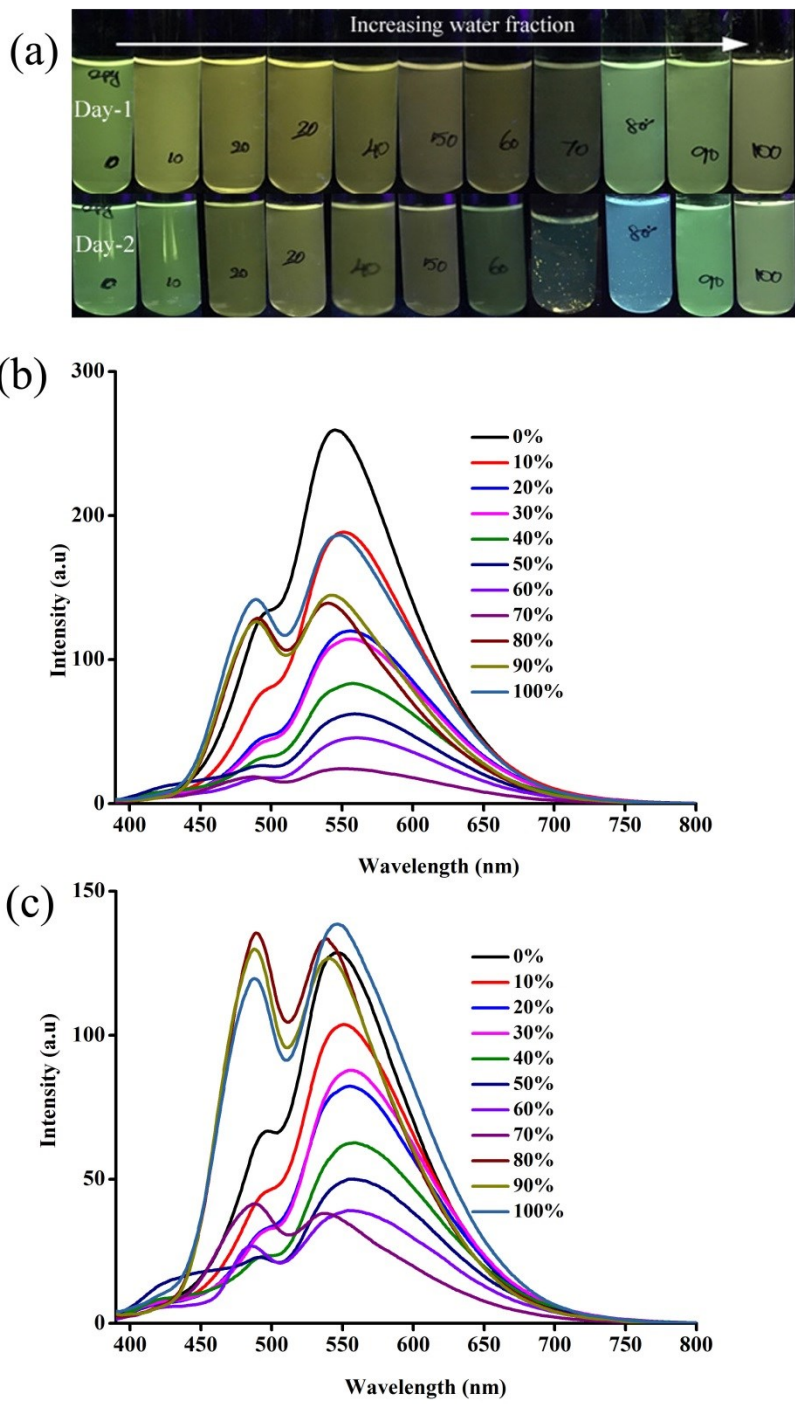


Fig. S5. AEE (a) digital fluorescence images and fluorescence spectra of **1** in (b) day 1 and (c) day 2.

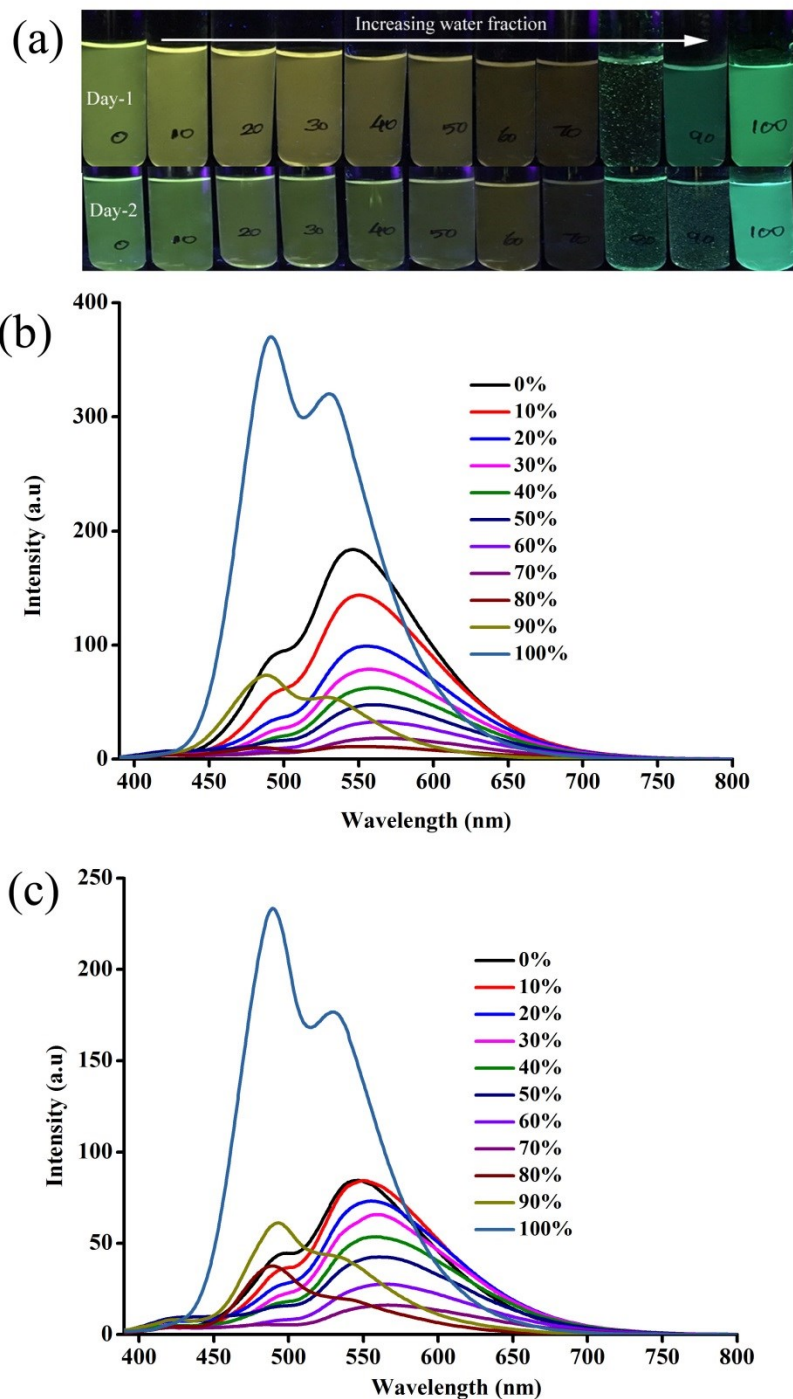


Fig. S6. AEE (a) digital fluorescence images and fluorescence spectra of **2** in (b) day 1 and (c) day 2.

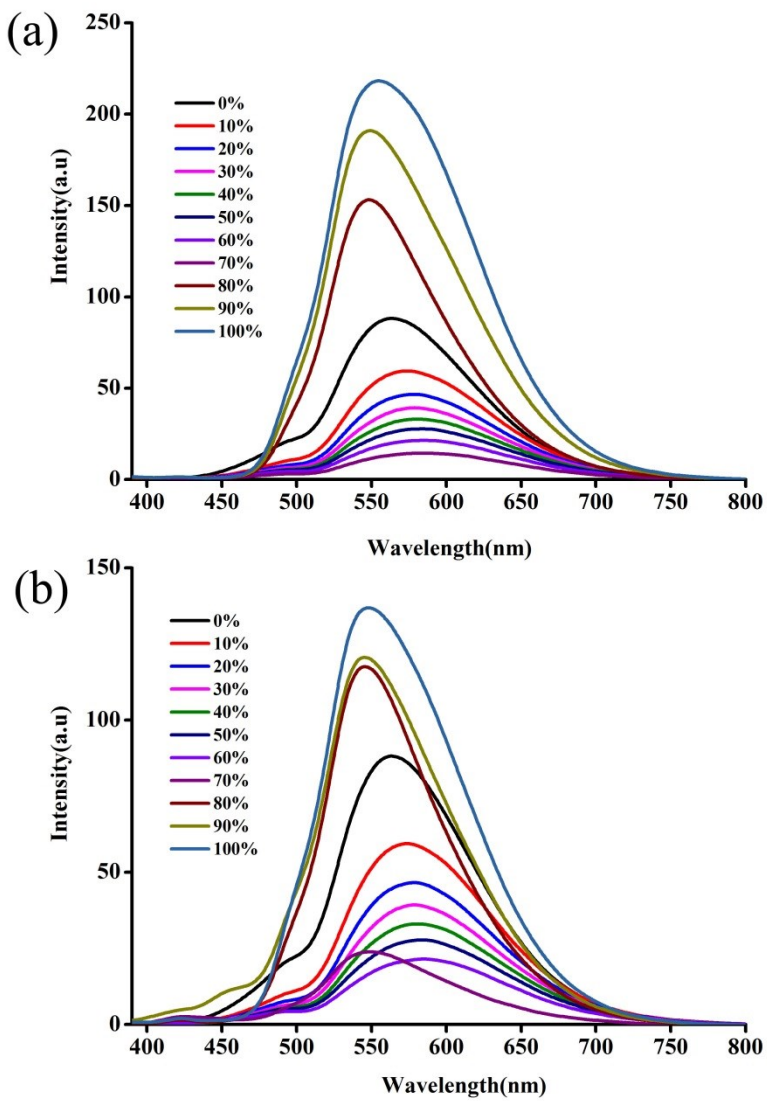


Fig. S7. AEE fluorescence spectra of **4** in (a) day 1 and (b) day 2.

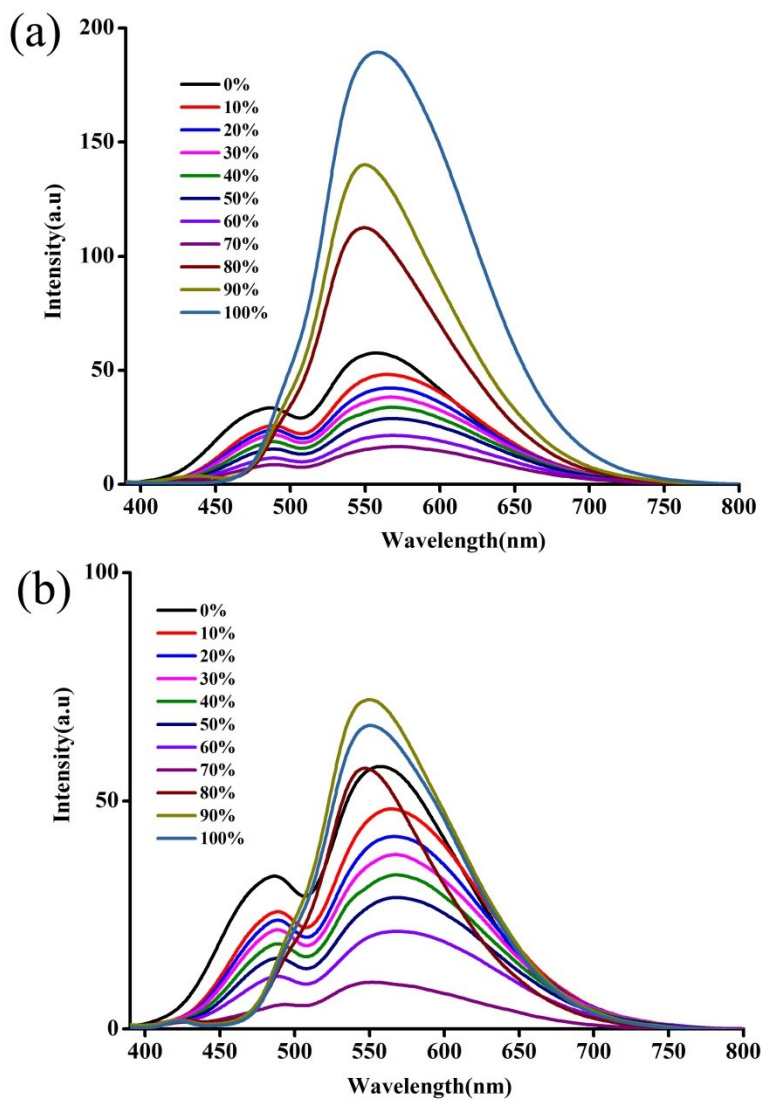


Fig. S8. AEE (a) digital fluorescence images and fluorescence spectra of **5** in (b) day 1 and (c) day 2.

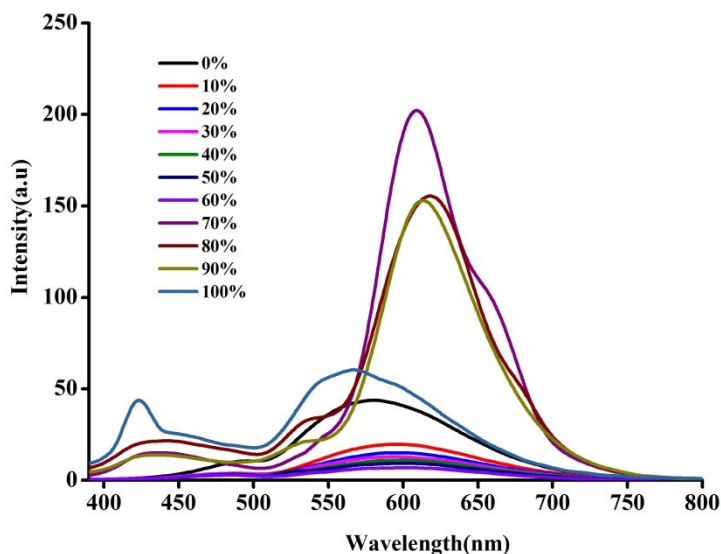


Fig. S9. AEE fluorescence spectra of **6** in day 2.

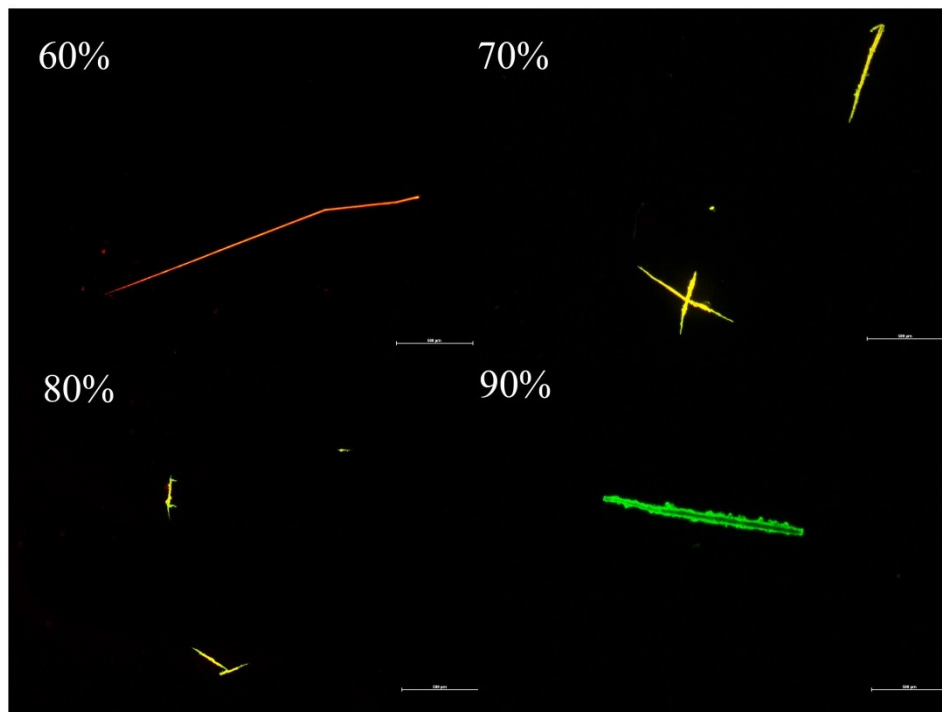


Fig. S10. Fluorescence microscopic images of **1** in different water fraction in CH<sub>3</sub>CN:water mixture in day 2.

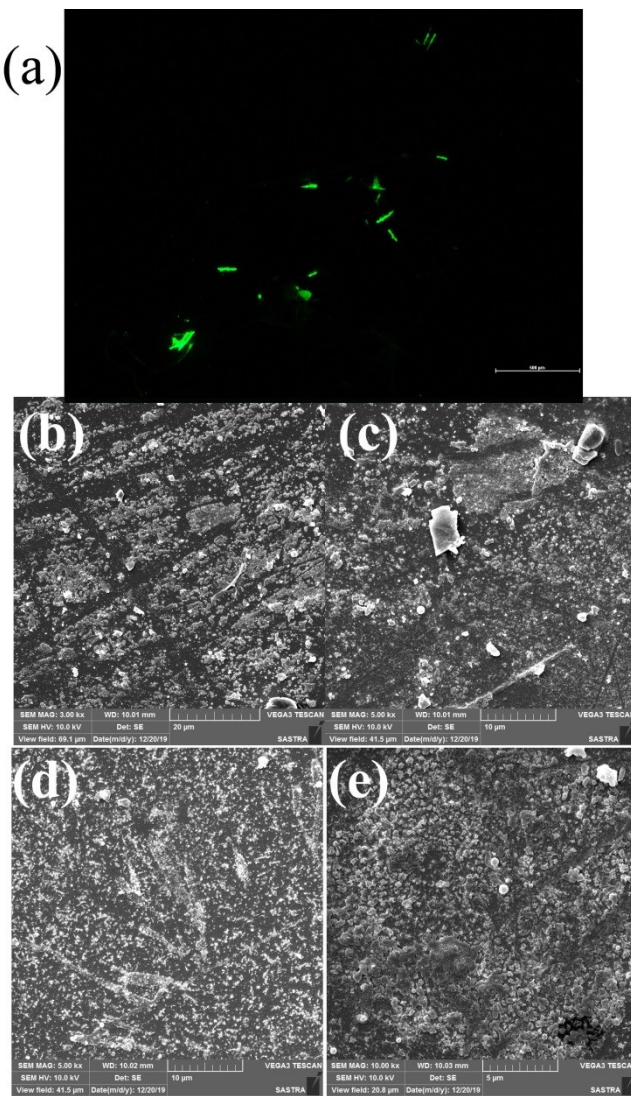


Fig. S11. (a) Fluorescence (100% water) and (b-e) scanning electron microscopic images of **1** in different water fraction in CH<sub>3</sub>CN:water mixture (b, c) 60% and (d, e) 100% in day 2.

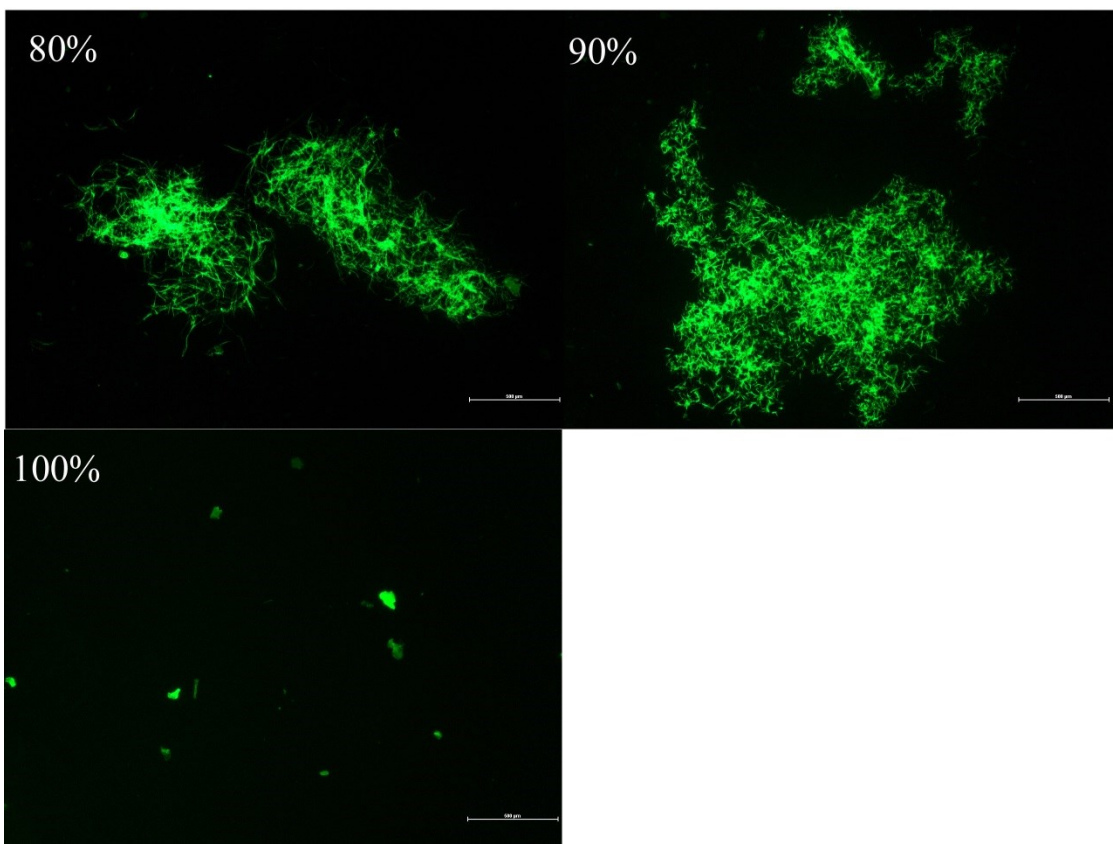


Fig. S12. Fluorescence microscopic images of **2** in different water fraction in CH<sub>3</sub>CN:water mixture in day 2.

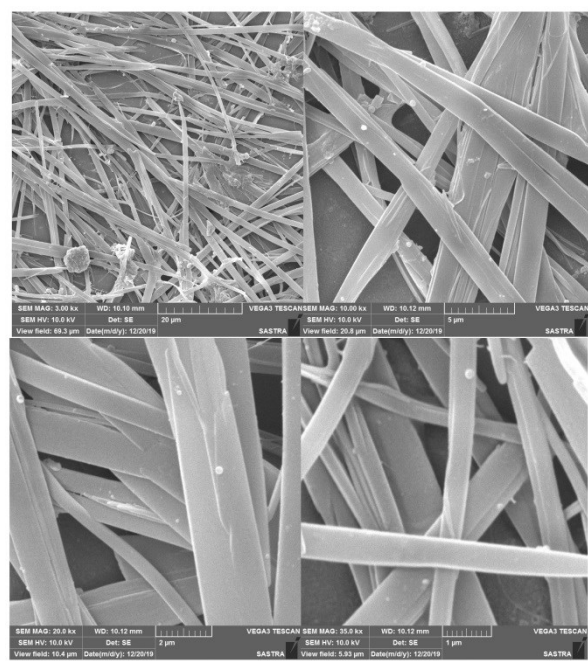


Fig. S13. Scanning electron microscopic images of **2** in 80% water fraction in CH<sub>3</sub>CN:water mixture in day 2.

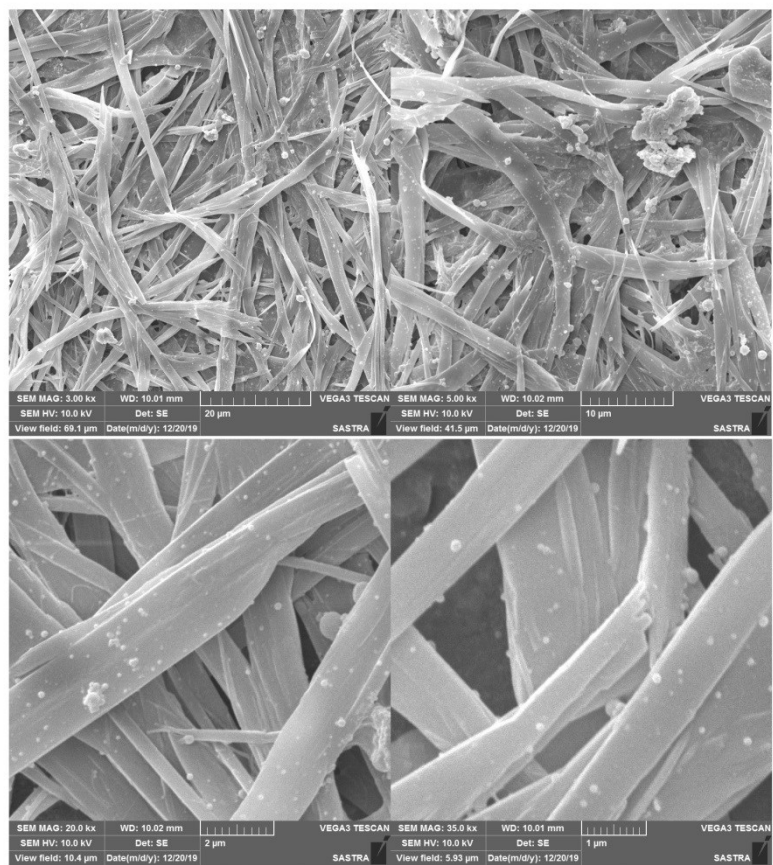


Fig. S14. Scanning electron microscopic images of **2** in 90% water fraction in  $\text{CH}_3\text{CN}$ :water mixture in day 2.

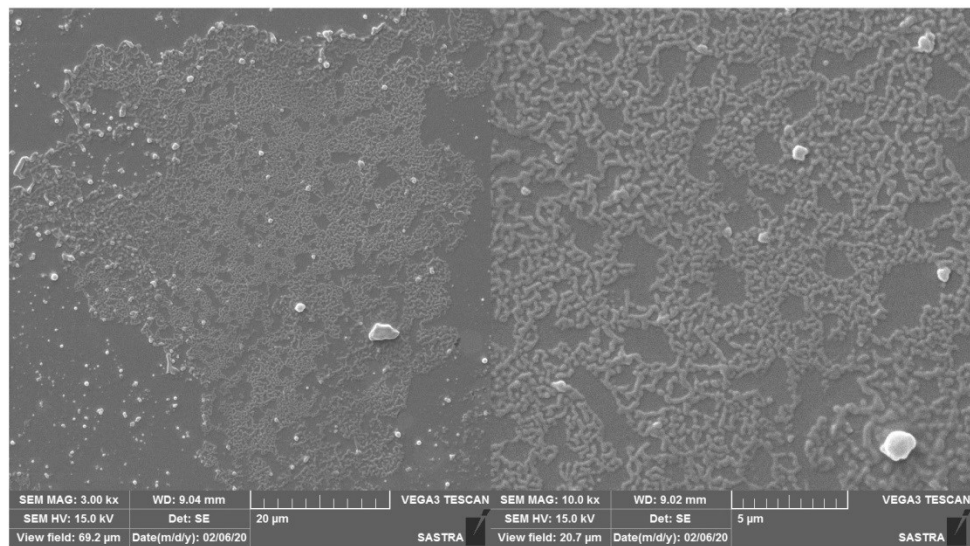


Fig. S15. Scanning electron microscopic images of **2** in 100% water fraction in  $\text{CH}_3\text{CN}$ :water mixture in day 2.

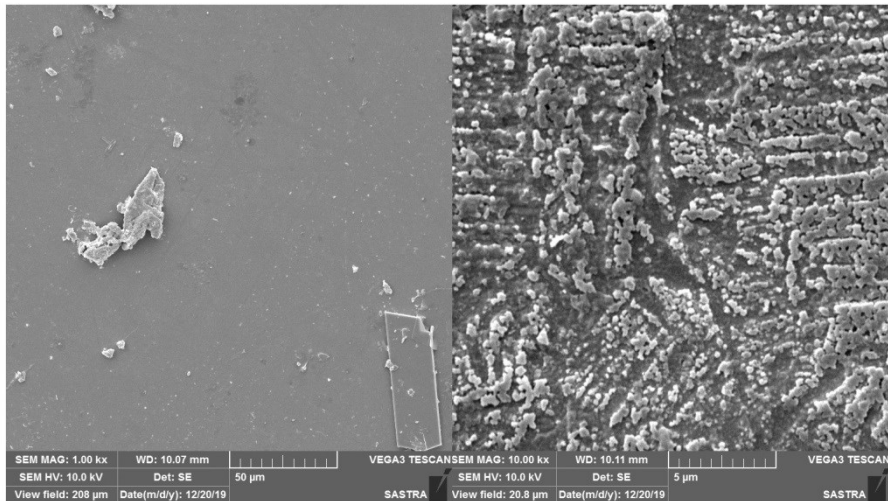


Fig. S16. Scanning electron microscopic images of **3** in 70% water fraction in  $\text{CH}_3\text{CN}$ :water mixture in day 2.

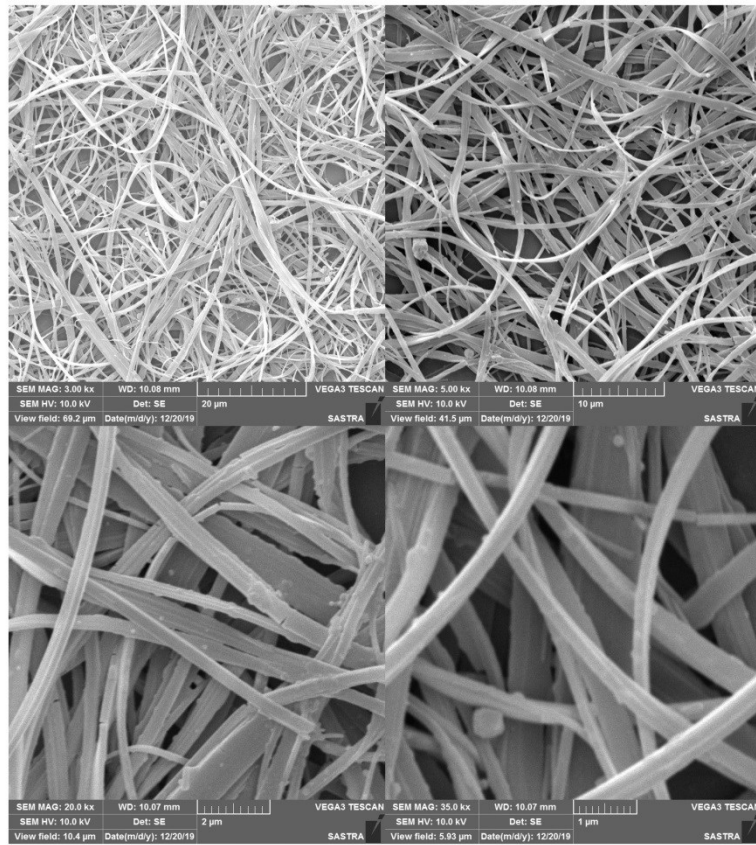


Fig. S17. Scanning electron microscopic images of **3** in 80% water fraction in  $\text{CH}_3\text{CN}$ :water mixture in day 2.

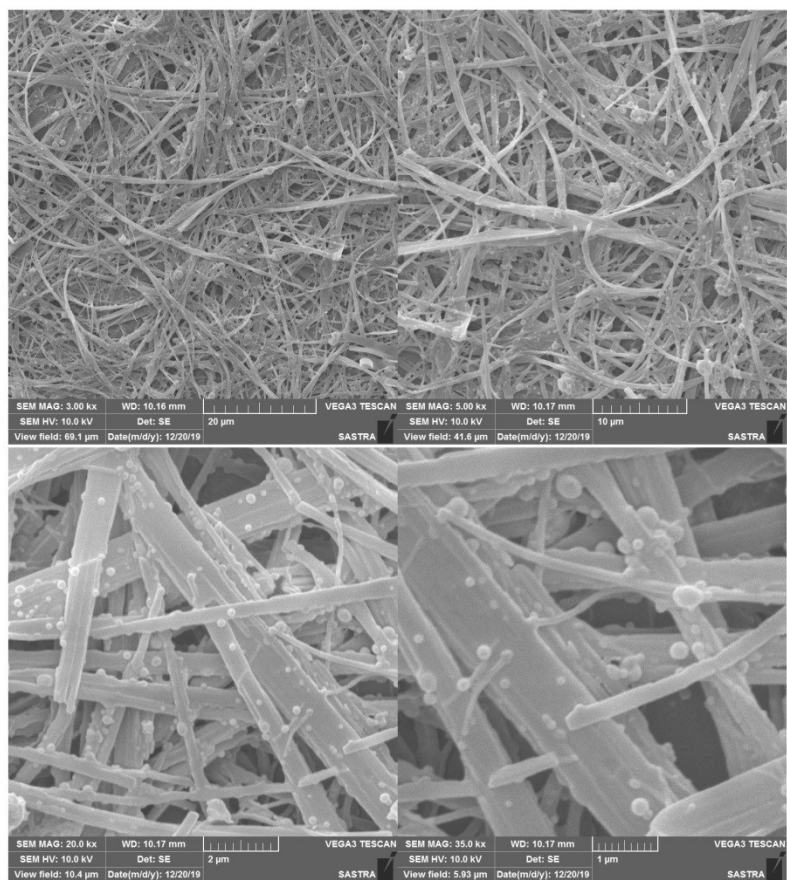


Fig. S18. Scanning electron microscopic images of **3** in 90% water fraction in  $\text{CH}_3\text{CN}$ :water mixture in day 2.

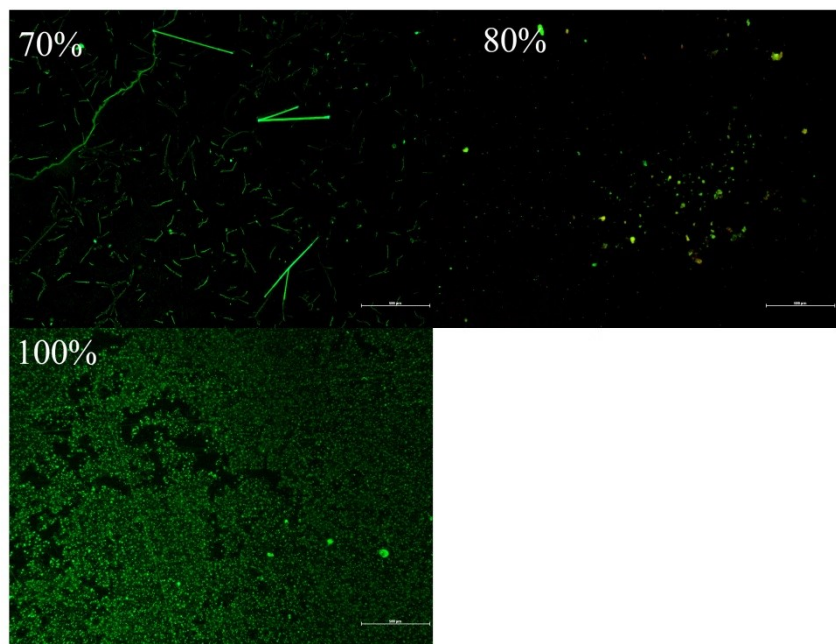


Fig. S19. Fluorescence microscopic images of **4** in different water fraction in  $\text{CH}_3\text{CN}$ :water mixture in day 2.

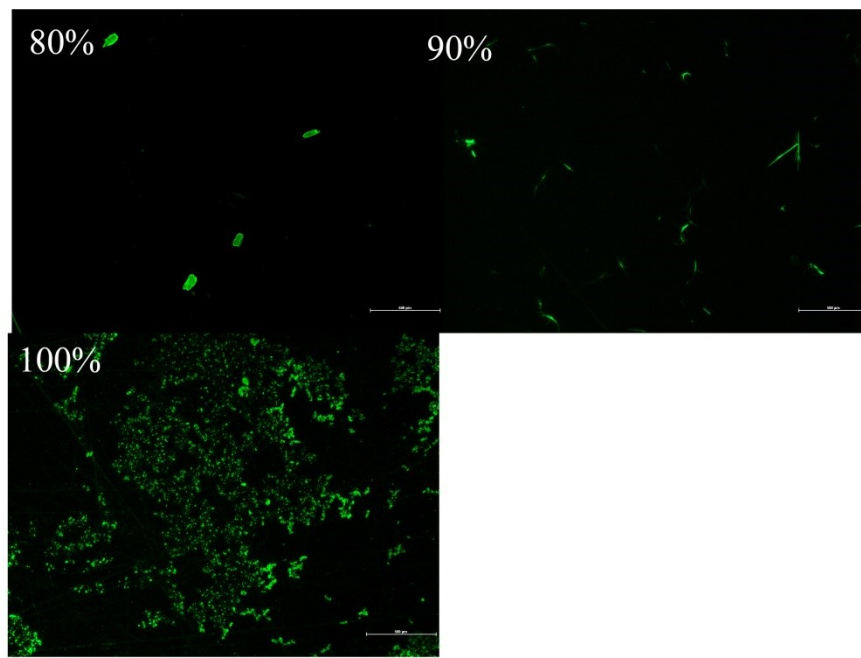


Fig. S20. Fluorescence microscopic images of **5** in different water fraction in CH<sub>3</sub>CN:water mixture in day 2.

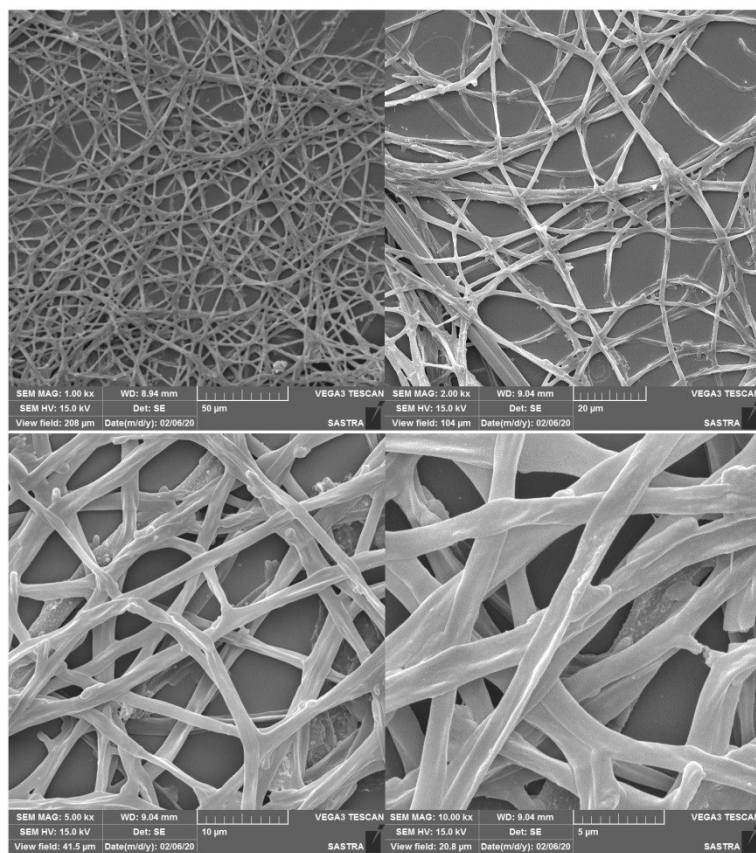


Fig. S21. Scanning electron microscopic images of **4** in 70% water fraction in CH<sub>3</sub>CN:water mixture in day 2.

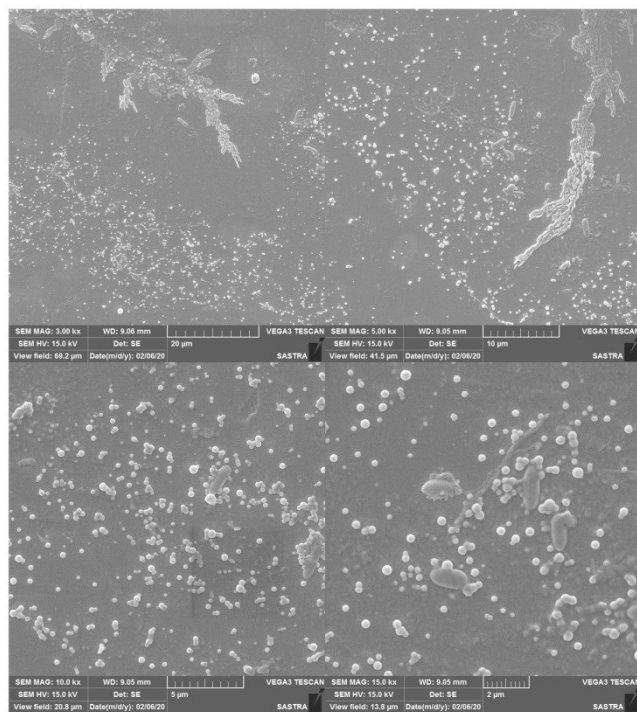


Fig. S22. Scanning electron microscopic images of **4** in 100% water fraction in CH<sub>3</sub>CN:water mixture in day 2.

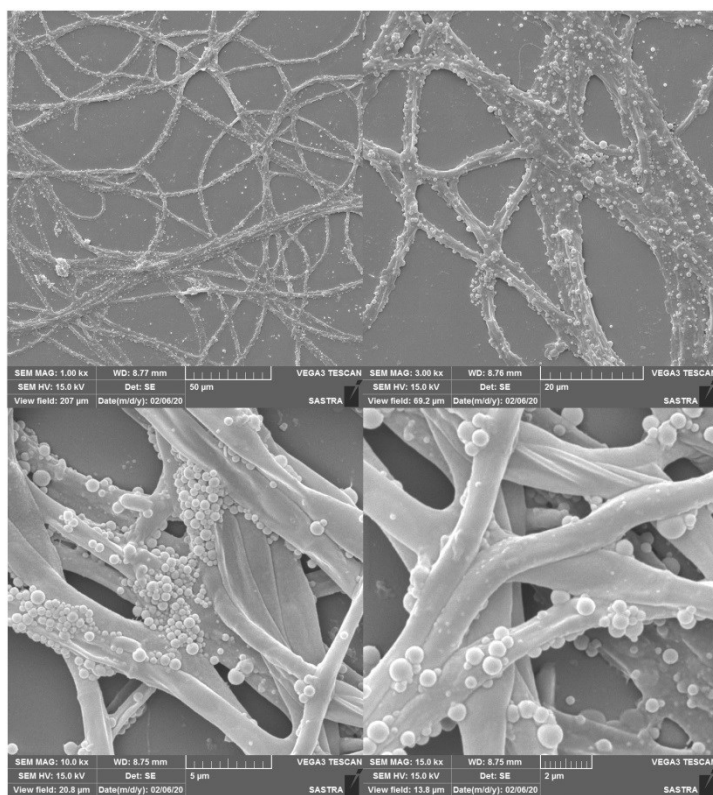


Fig. S23. Scanning electron microscopic images of **5** in 100% water fraction in CH<sub>3</sub>CN:water mixture in day 2.

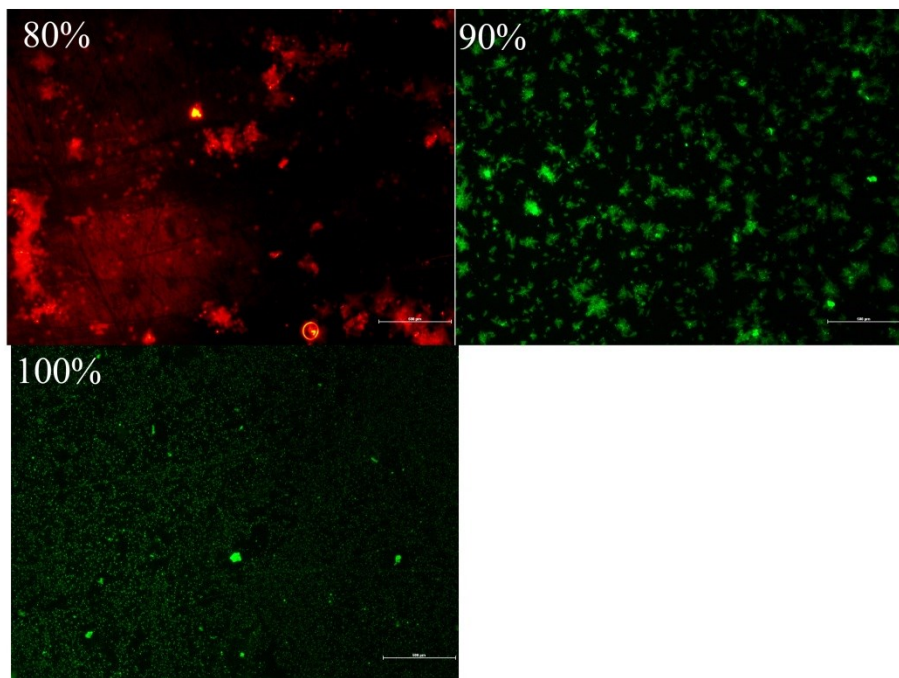


Fig. S24. Fluorescence microscopic images of **6** in different water fraction in CH<sub>3</sub>CN:water mixture in day 2.

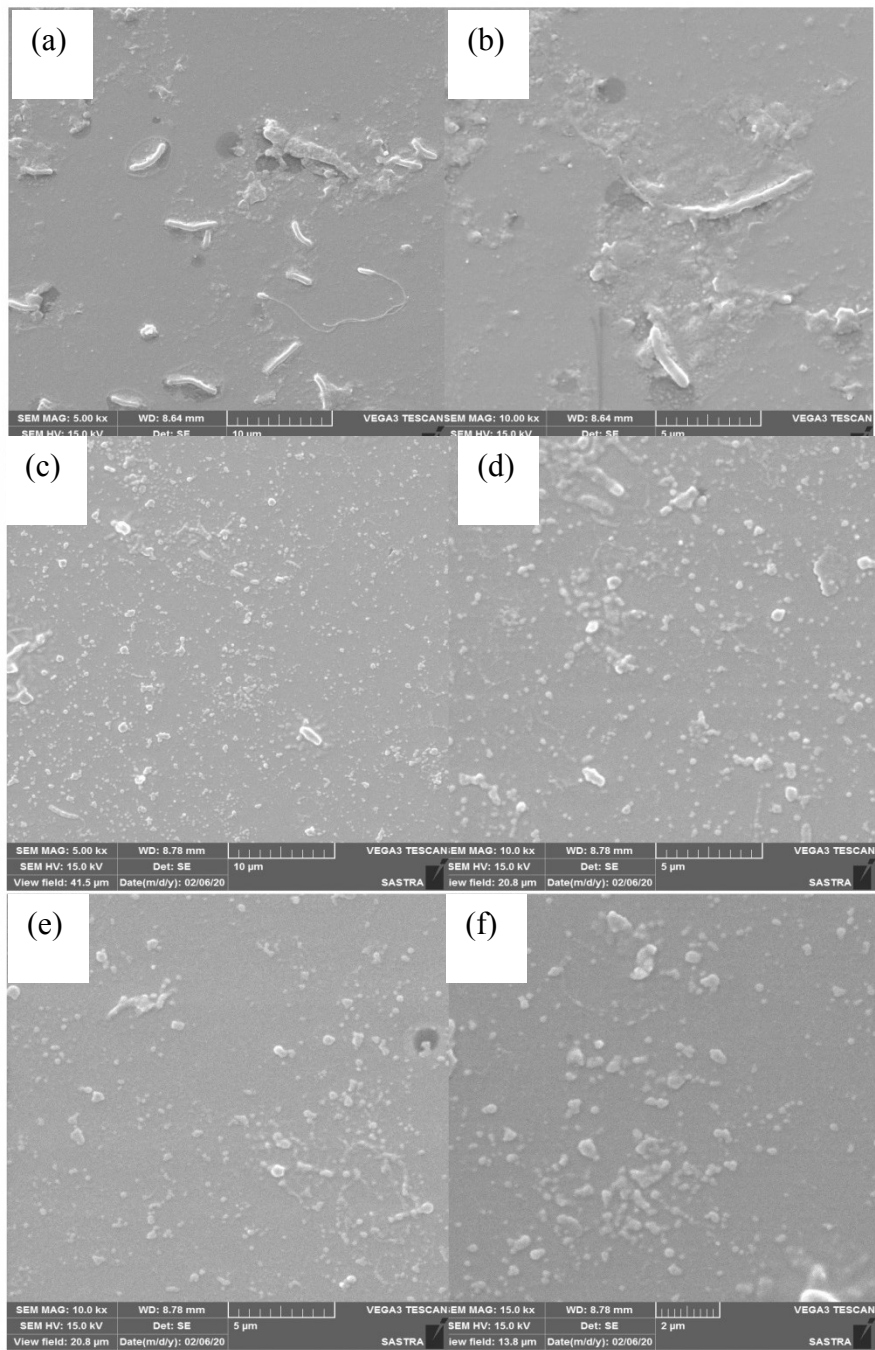
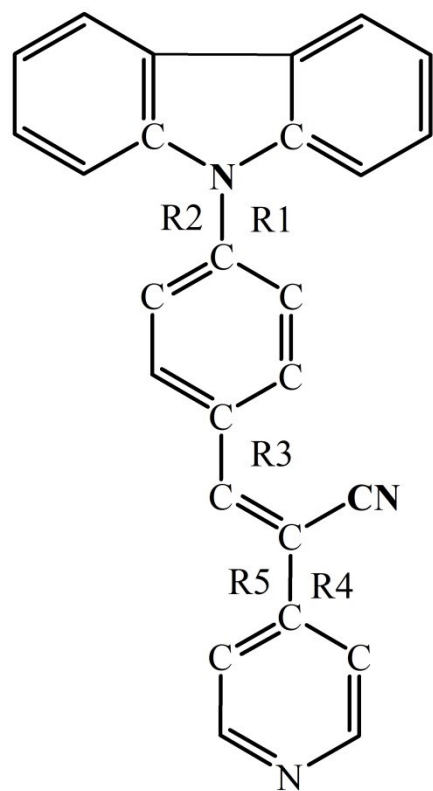


Fig. S25. Scanning electron microscopic images of **6** in (a,b) 80% and (c-f) 100% water fraction in  $\text{CH}_3\text{CN}$ :water mixture in day 2.

Table S2. Molecular conformational changes observed in the crystal lattices of **1-4** and **6**.



	Torsion angle ( $\tau$ )				
	R1	R2	R3	R4	R5
1-G	43.81	46.57	18.51	0.55	1.94
1-O	43.98	46.39	18.30	0.75	2.14
2	50.54	53.95	19.22	6.99	8.22
3-G	42.45, 44.25	48.59, 35.30	16.76, 23.25	23.46, 4.52	8.54, 21.14
3-Y	41.93, 43.40	48.75, 35.33	16.66, 23.75	23.50, 4.86	7.88, 20.96
4	25.24	35.79	3.82	8.58	6.82
6	32.19	30.25	19.61	28.78	33.95

Table S3. Crystal data and structure refinement for **1-G**.

Identification code	1-G		
Empirical formula	$C_{26}H_{17}N_3$		
Formula weight	371.42		
Temperature	220(2) K		
Wavelength	0.630 Å		
Crystal system	Monoclinic		
Space group	P2 <sub>1</sub> /c		
Unit cell dimensions	$a = 14.957(3)$ Å	$\alpha = 90^\circ$ .	
	$b = 17.427(4)$ Å	$\beta = 95.41(3)^\circ$ .	
	$c = 7.1320(14)$ Å	$\gamma = 90^\circ$ .	
Volume	1850.7(6) Å <sup>3</sup>		
Z	4		
Density (calculated)	1.333 Mg/m <sup>3</sup>		
Absorption coefficient	0.063 mm <sup>-1</sup>		
F(000)	776		
Crystal size	0.159 x 0.125 x 0.097 mm <sup>3</sup>		
Theta range for data collection	1.212 to 25.498°.		
Index ranges	-20≤h≤20, -23≤k≤23, -9≤l≤9		
Reflections collected	17634		
Independent reflections	4955 [R(int) = 0.0608]		
Completeness to theta = 22.210°	100.0 %		
Absorption correction	Empirical		
Max. and min. transmission	1.000 and 0.963		
Refinement method	Full-matrix least-squares on F <sup>2</sup>		
Data / restraints / parameters	4955 / 0 / 262		
Goodness-of-fit on F <sup>2</sup>	1.123		
Final R indices [I>2sigma(I)]	R1 = 0.0549, wR2 = 0.1641		
R indices (all data)	R1 = 0.0642, wR2 = 0.1698		
Extinction coefficient	n/a		
Largest diff. peak and hole	0.464 and -0.335 e.Å <sup>-3</sup>		

Table S4. Crystal data and structure refinement for **1-O**.

Identification code	1-O		
Empirical formula	$C_{26}H_{17}N_3$		
Formula weight	371.42		
Temperature	220(2) K		
Wavelength	0.630 Å		
Crystal system	Monoclinic		
Space group	P2 <sub>1</sub> /c		
Unit cell dimensions	$a = 14.955(3)$ Å	$\alpha = 90^\circ$ .	
	$b = 17.421(4)$ Å	$\beta = 95.38(3)^\circ$ .	
	$c = 7.1320(14)$ Å	$\gamma = 90^\circ$ .	
Volume	$1849.9(6)$ Å <sup>3</sup>		
Z	4		
Density (calculated)	1.334 Mg/m <sup>3</sup>		
Absorption coefficient	0.063 mm <sup>-1</sup>		
F(000)	776		
Crystal size	$0.105 \times 0.094 \times 0.074$ mm <sup>3</sup>		
Theta range for data collection	1.212 to 25.497°.		
Index ranges	$-20 \leq h \leq 20, -23 \leq k \leq 23, -9 \leq l \leq 9$		
Reflections collected	17419		
Independent reflections	4953 [R(int) = 0.0630]		
Completeness to theta = 22.210°	100.0 %		
Absorption correction	Empirical		
Max. and min. transmission	1.000 and 0.961		
Refinement method	Full-matrix least-squares on F <sup>2</sup>		
Data / restraints / parameters	4953 / 0 / 262		
Goodness-of-fit on F <sup>2</sup>	1.039		
Final R indices [I>2sigma(I)]	R1 = 0.0512, wR2 = 0.1398		
R indices (all data)	R1 = 0.0646, wR2 = 0.1462		
Extinction coefficient	n/a		
Largest diff. peak and hole	0.346 and -0.352 e.Å <sup>-3</sup>		

Table S5. Crystal data and structure refinement for **2**.

Identification code	<b>2</b>	
Empirical formula	C <sub>26</sub> H <sub>17</sub> N <sub>3</sub>	
Formula weight	371.42	
Temperature	220(2) K	
Wavelength	0.610 Å	
Crystal system	Orthorhombic	
Space group	Pna2 <sub>1</sub>	
Unit cell dimensions	a = 21.773(4) Å b = 6.9330(14) Å c = 12.578(3) Å	α = 90°. β = 90°. γ = 90°.
Volume	1898.7(7) Å <sup>3</sup>	
Z	4	
Density (calculated)	1.299 Mg/m <sup>3</sup>	
Absorption coefficient	0.058 mm <sup>-1</sup>	
F(000)	776	
Crystal size	0.065 x 0.027 x 0.012 mm <sup>3</sup>	
Theta range for data collection	1.605 to 24.996°.	
Index ranges	-30<=h<=30, -9<=k<=9, -17<=l<=17	
Reflections collected	18632	
Independent reflections	5280 [R(int) = 0.0862]	
Completeness to theta = 21.469°	100.0 %	
Absorption correction	Empirical	
Max. and min. transmission	1.000 and 0.829	
Refinement method	Full-matrix least-squares on F <sup>2</sup>	
Data / restraints / parameters	5280 / 1 / 263	
Goodness-of-fit on F <sup>2</sup>	0.927	
Final R indices [I>2sigma(I)]	R1 = 0.0573, wR2 = 0.1388	
R indices (all data)	R1 = 0.0924, wR2 = 0.1551	
Absolute structure parameter	1(6)	
Extinction coefficient	n/a	
Largest diff. peak and hole	0.316 and -0.195 e.Å <sup>-3</sup>	

Table S6. Crystal data and structure refinement for **3-G**.

Identification code	3-G	
Empirical formula	$C_{26}H_{17}N_3$	
Formula weight	371.42	
Temperature	220(2) K	
Wavelength	0.630 Å	
Crystal system	Monoclinic	
Space group	P2 <sub>1</sub> /n	
Unit cell dimensions	$a = 17.613(4)$ Å	$\alpha = 90^\circ$ .
	$b = 7.8670(16)$ Å	$\beta = 102.53(3)^\circ$ .
	$c = 27.784(6)$ Å	$\gamma = 90^\circ$ .
Volume	3758.1(14) Å <sup>3</sup>	
Z	8	
Density (calculated)	1.313 Mg/m <sup>3</sup>	
Absorption coefficient	0.062 mm <sup>-1</sup>	
F(000)	1552	
Crystal size	0.073 x 0.068 x 0.009 mm <sup>3</sup>	
Theta range for data collection	1.331 to 25.499°.	
Index ranges	-24≤h≤24, -10≤k≤10, -37≤l≤37	
Reflections collected	35185	
Independent reflections	10047 [R(int) = 0.1256]	
Completeness to theta = 22.210°	100.0 %	
Absorption correction	Empirical	
Max. and min. transmission	1.000 and 0.964	
Refinement method	Full-matrix least-squares on F <sup>2</sup>	
Data / restraints / parameters	10047 / 0 / 523	
Goodness-of-fit on F <sup>2</sup>	0.798	
Final R indices [I>2sigma(I)]	R1 = 0.0586, wR2 = 0.1190	
R indices (all data)	R1 = 0.1478, wR2 = 0.1410	
Extinction coefficient	n/a	
Largest diff. peak and hole	0.210 and -0.290 e.Å <sup>-3</sup>	

Table S7. Crystal data and structure refinement for **3-Y**.

Identification code	3-Y		
Empirical formula	$C_{52}H_{34}N_6$		
Formula weight	742.85		
Temperature	220(2) K		
Wavelength	0.610 Å		
Crystal system	Monoclinic		
Space group	P2 <sub>1</sub> /n		
Unit cell dimensions	$a = 17.595(4)$ Å	$\alpha = 90^\circ$ .	
	$b = 7.8670(16)$ Å	$\beta = 102.57(3)^\circ$ .	
	$c = 27.780(6)$ Å	$\gamma = 90^\circ$ .	
Volume	3753.1(14) Å <sup>3</sup>		
Z	4		
Density (calculated)	1.315 Mg/m <sup>3</sup>		
Absorption coefficient	0.058 mm <sup>-1</sup>		
F(000)	1552		
Crystal size	0.064 x 0.031 x 0.009 mm <sup>3</sup>		
Theta range for data collection	1.289 to 25.000°.		
Index ranges	-24≤h≤24, -10≤k≤10, -38≤l≤38		
Reflections collected	37387		
Independent reflections	10399 [R(int) = 0.1493]		
Completeness to theta = 21.469°	99.8 %		
Absorption correction	Empirical		
Max. and min. transmission	1.000 and 0.746		
Refinement method	Full-matrix least-squares on F <sup>2</sup>		
Data / restraints / parameters	10399 / 12 / 524		
Goodness-of-fit on F <sup>2</sup>	0.791		
Final R indices [I>2sigma(I)]	R1 = 0.0580, wR2 = 0.1217		
R indices (all data)	R1 = 0.1789, wR2 = 0.1550		
Extinction coefficient	0.0095(8)		
Largest diff. peak and hole	0.234 and -0.200 e.Å <sup>-3</sup>		

**Table S8. Crystal data and structure refinement for 4.**

Identification code	4	
Empirical formula	C26 H19 N3	
Formula weight	373.44	
Temperature	220(2) K	
Wavelength	0.650 Å	
Crystal system	Orthorhombic	
Space group	Pca2 <sub>1</sub>	
Unit cell dimensions	a = 27.195(5) Å b = 7.8540(16) Å c = 9.4070(19) Å	α= 90°. β= 90°. γ = 90°.
Volume	2009.2(7) Å <sup>3</sup>	
Z	4	
Density (calculated)	1.235 Mg/m <sup>3</sup>	
Absorption coefficient	0.061 mm <sup>-1</sup>	
F(000)	784	
Crystal size	0.065 x 0.059 x 0.043 mm <sup>3</sup>	
Theta range for data collection	2.372 to 25.999°.	
Index ranges	-36<=h<=36, -10<=k<=10, -11<=l<=11	
Reflections collected	18147	
Independent reflections	4952 [R(int) = 0.0564]	
Completeness to theta = 22.955°	97.2 %	
Absorption correction	Empirical	
Max. and min. transmission	1.000 and 0.897	
Refinement method	Full-matrix least-squares on F <sup>2</sup>	
Data / restraints / parameters	4952 / 7 / 263	
Goodness-of-fit on F <sup>2</sup>	1.076	
Final R indices [I>2sigma(I)]	R1 = 0.0434, wR2 = 0.1149	
R indices (all data)	R1 = 0.0478, wR2 = 0.1174	
Absolute structure parameter	0(4)	
Extinction coefficient	n/a	
Largest diff. peak and hole	0.236 and -0.202 e.Å <sup>-3</sup>	

Table S9. Crystal data and structure refinement for **6**.

Identification code	6	
Empirical formula	C <sub>26</sub> H <sub>19</sub> N <sub>3</sub>	
Formula weight	373.44	
Temperature	220(2) K	
Wavelength	0.610 Å	
Crystal system	Orthorhombic	
Space group	<i>Pbcn</i>	
Unit cell dimensions	a = 24.522(5) Å b = 10.288(2) Å c = 15.547(3) Å	α = 90°. β = 90°. γ = 90°.
Volume	3922.2(14) Å <sup>3</sup>	
Z	8	
Density (calculated)	1.265 Mg/m <sup>3</sup>	
Absorption coefficient	0.056 mm <sup>-1</sup>	
F(000)	1568	
Crystal size	0.107 x 0.099 x 0.043 mm <sup>3</sup>	
Theta range for data collection	1.842 to 25.000°.	
Index ranges	-33<=h<=33, -14<=k<=14, -21<=l<=21	
Reflections collected	37251	
Independent reflections	5442 [R(int) = 0.0691]	
Completeness to theta = 21.469°	99.8 %	
Absorption correction	Empirical	
Max. and min. transmission	1.000 and 0.971	
Refinement method	Full-matrix least-squares on F <sup>2</sup>	
Data / restraints / parameters	5442 / 0 / 262	
Goodness-of-fit on F <sup>2</sup>	1.119	
Final R indices [I>2sigma(I)]	R1 = 0.0586, wR2 = 0.1722	
R indices (all data)	R1 = 0.0724, wR2 = 0.1796	
Extinction coefficient	n/a	
Largest diff. peak and hole	0.464 and -0.355 e.Å <sup>-3</sup>	

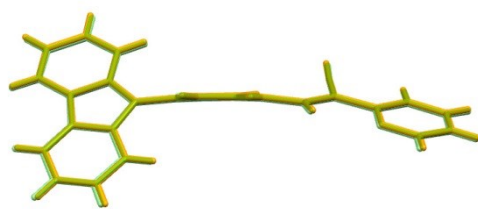


Fig. S26. Superimposed molecular conformaton of **1-G** and **1-O** polymorphs.

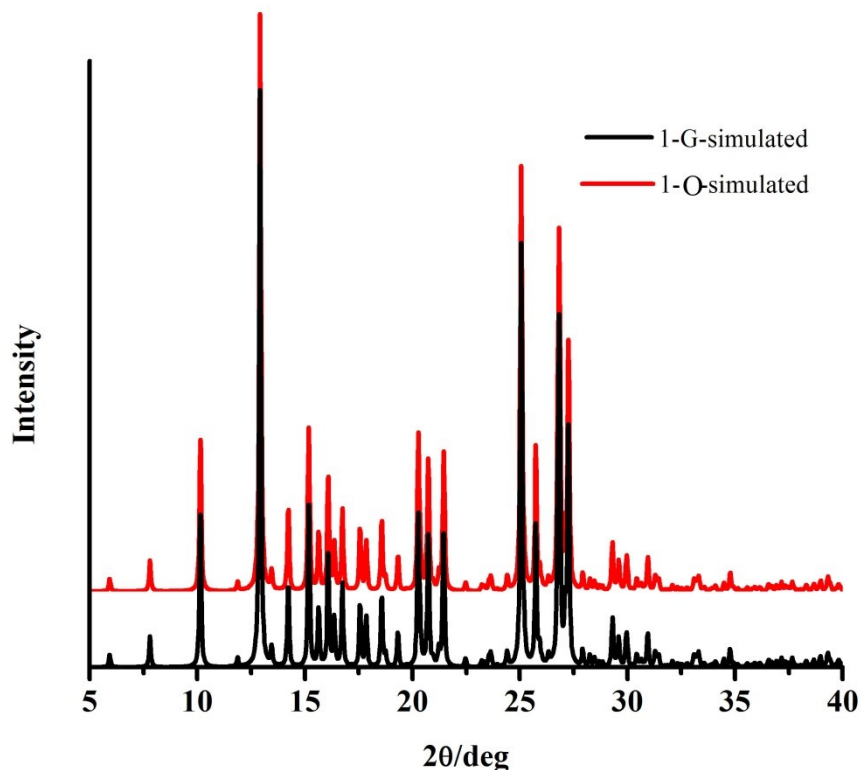


Fig. S27. Simulated PXRD pattern of **1-G** and **1-O**.

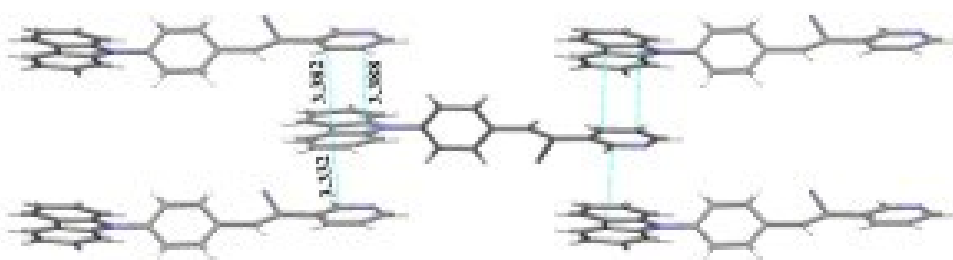


Fig. S28. Intermolecular interactions in the crystal lattice of **2**.

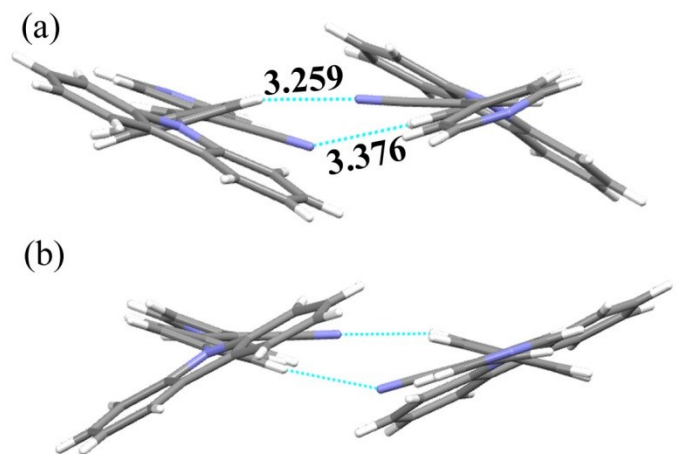


Fig. S29. Comparison of dimer formation in the crystal lattice of (a) **3-G** and (b) **3-Y**.

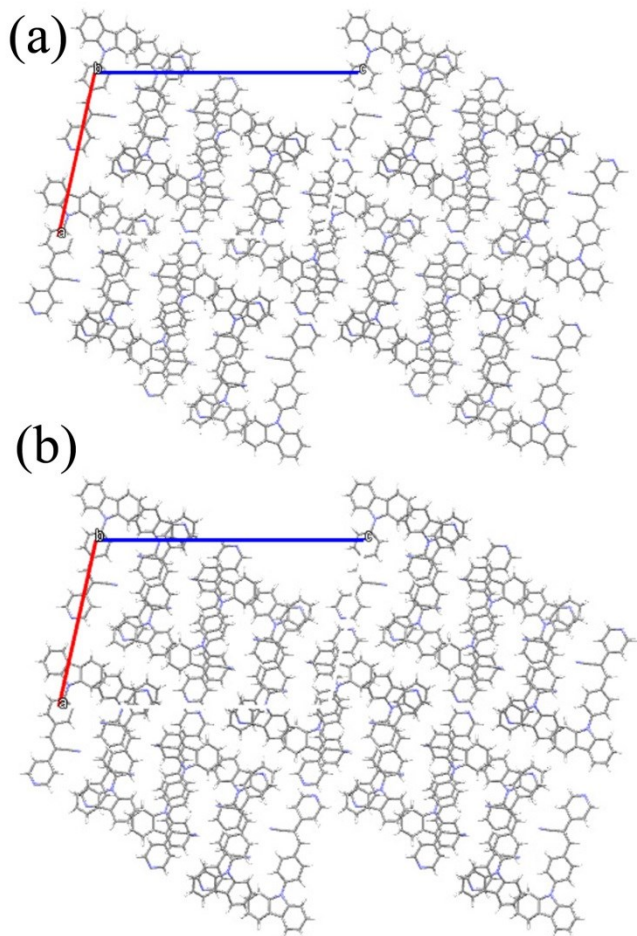


Fig. S30. Molecular packing in the crystal lattice of (a) **3-G** and (b) **3-Y**.

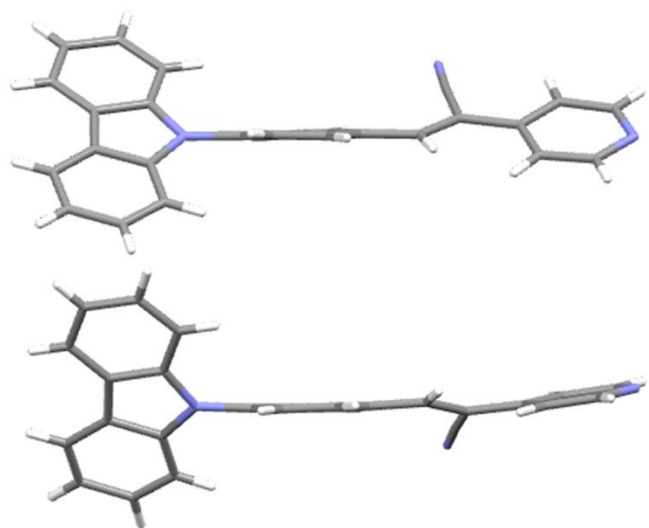


Fig. S31. Molecular conformation of molecules occupied in the asymmetric of (a) **3-G/3-Y**.

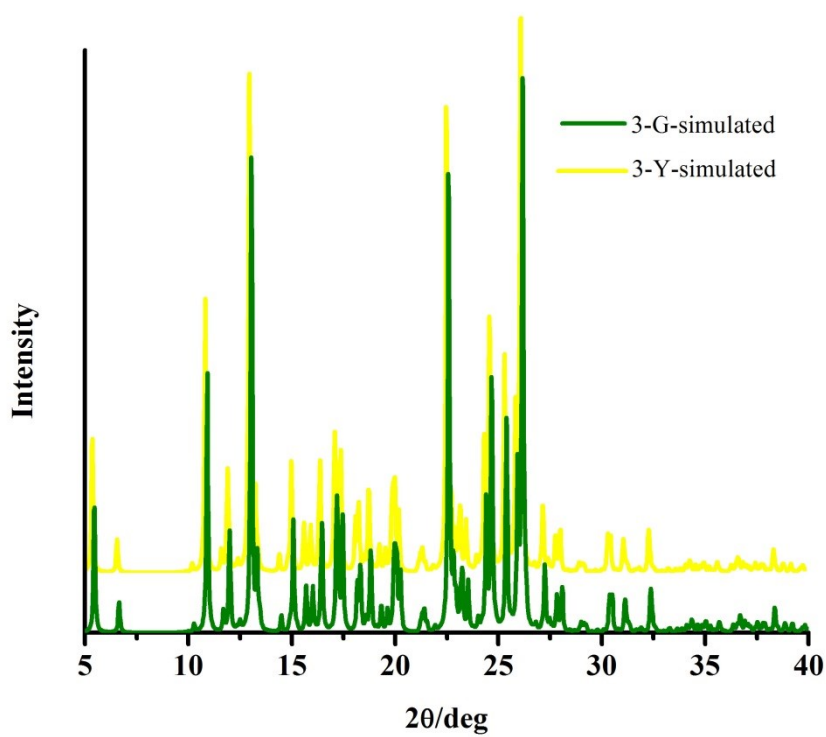


Fig. S32. Simulated PXRD pattern of **3-G** and **3-Y**.

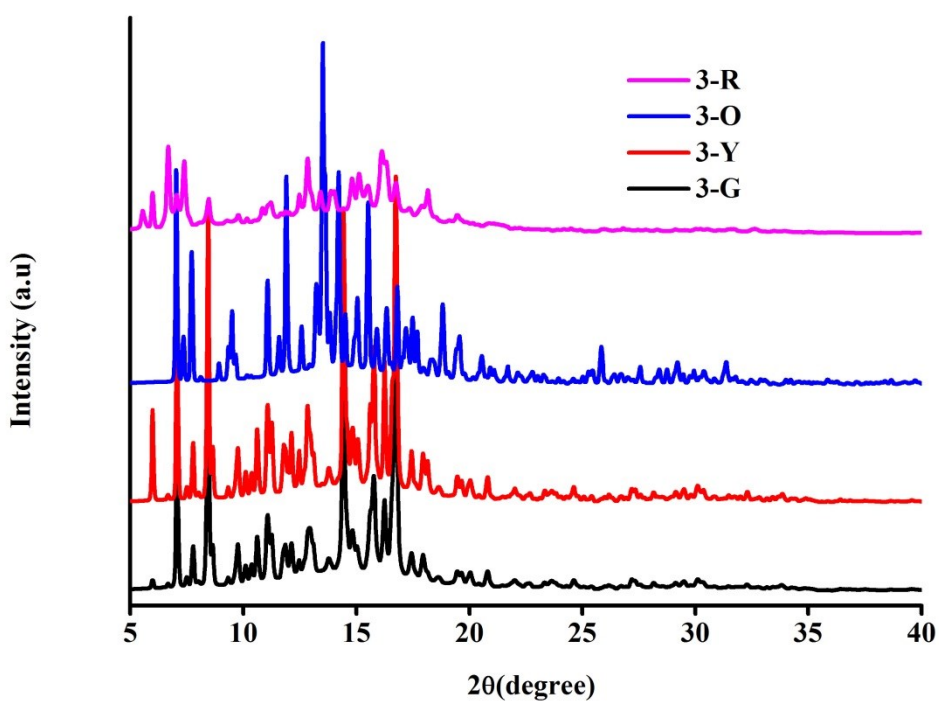


Fig. S33. PXRD pattern of **3-G**, **3-Y**, **3-O** and **3-R**.

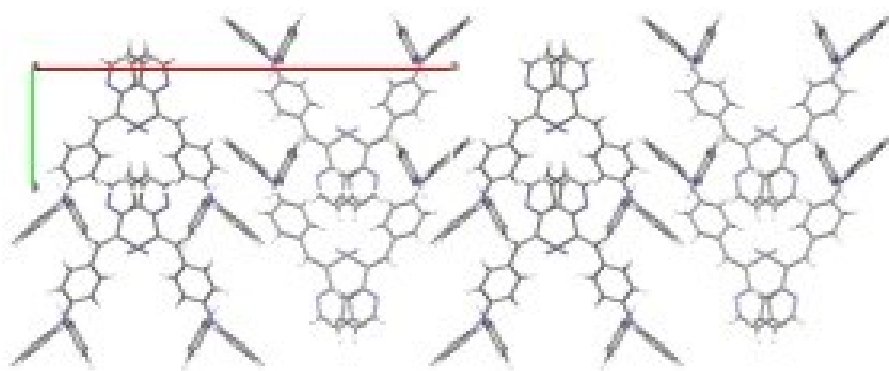


Fig. S34. Molecular packing in the crystal lattice of **4**.

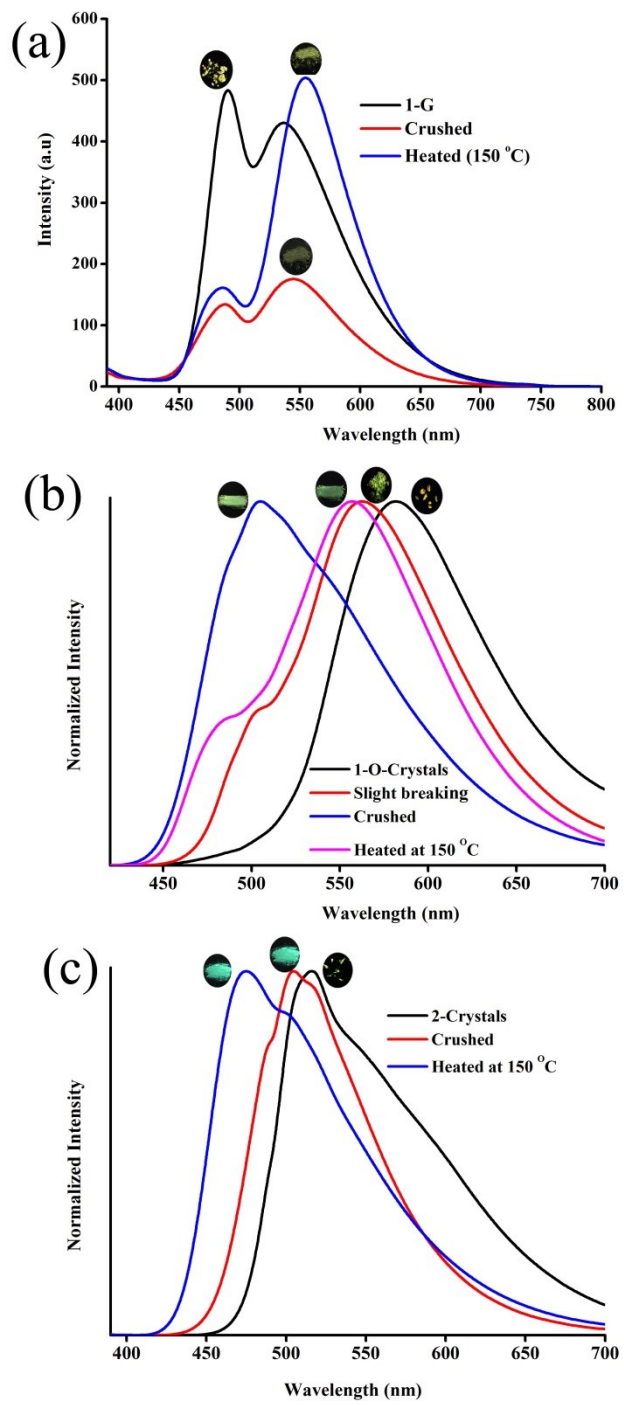


Fig. S35. MFC of **1-G**, **1-O** and **2**.

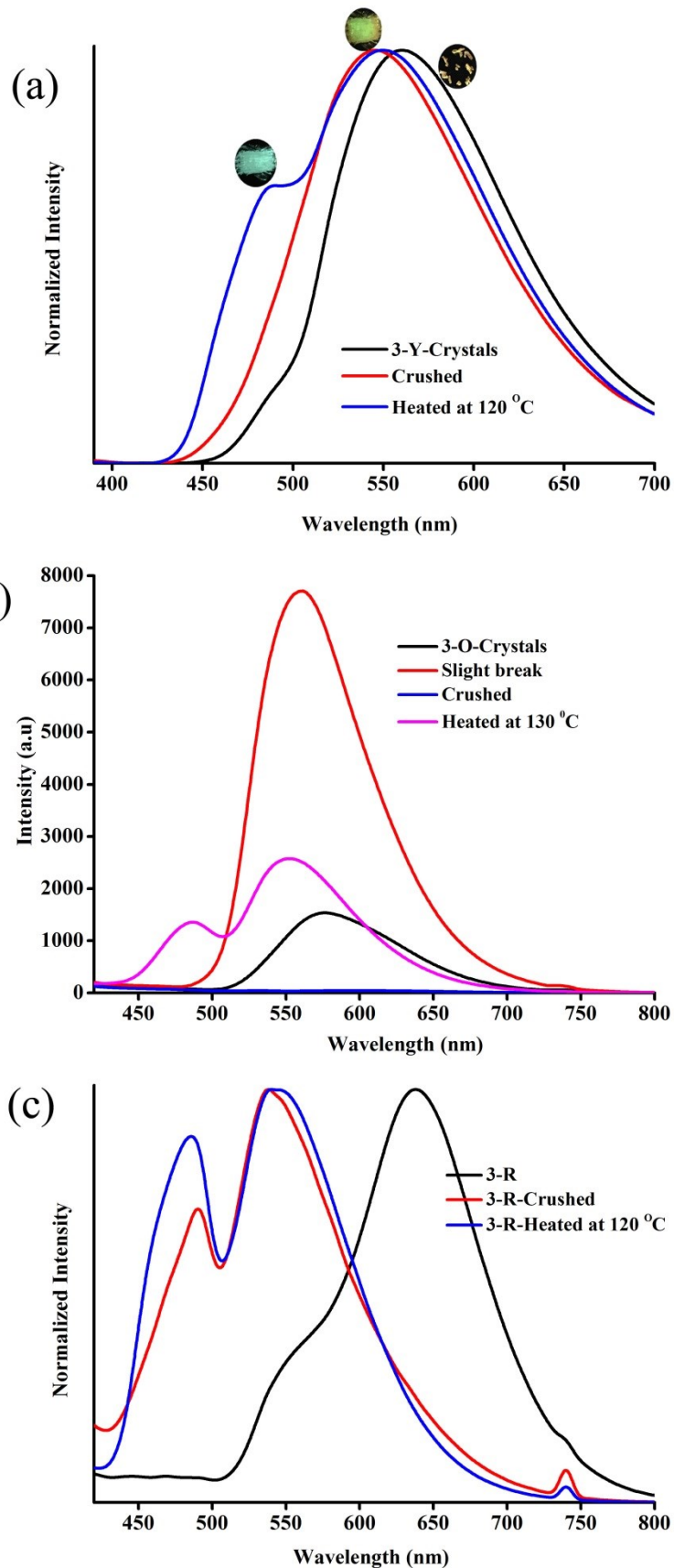


Fig. S36. MFC of (a) 3-Y, (b) 3-O and (c) 3-R.

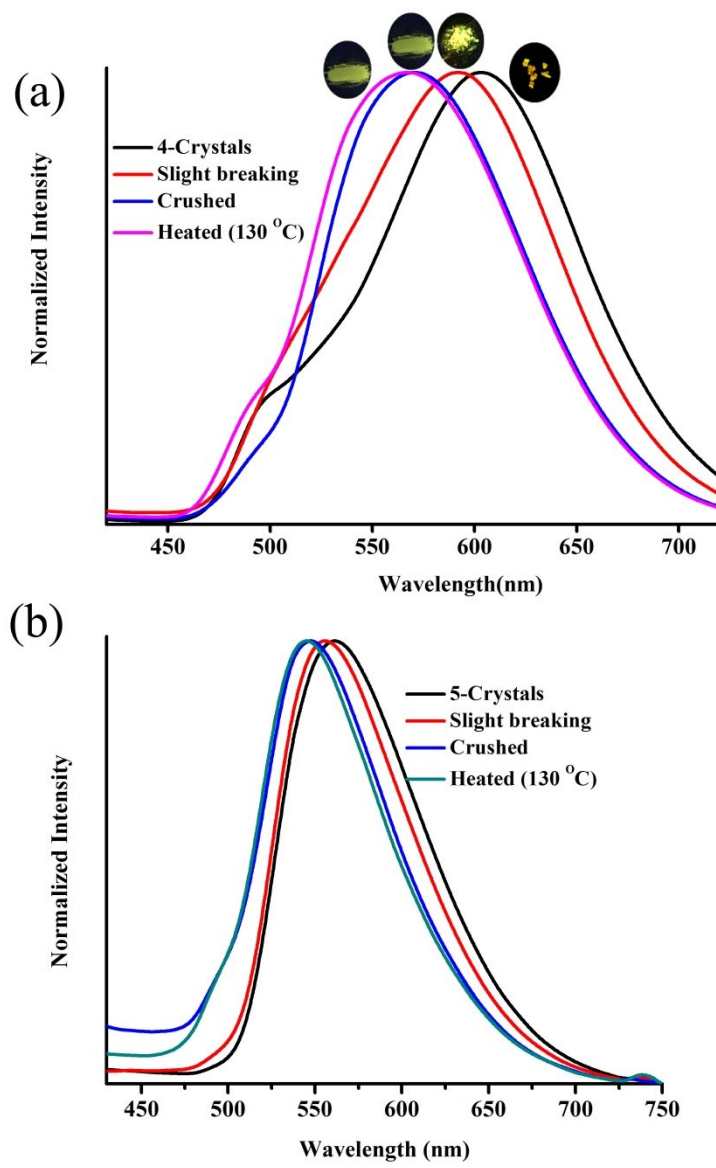


Fig. S37. MFC of (a) **4** and (b) **5**.

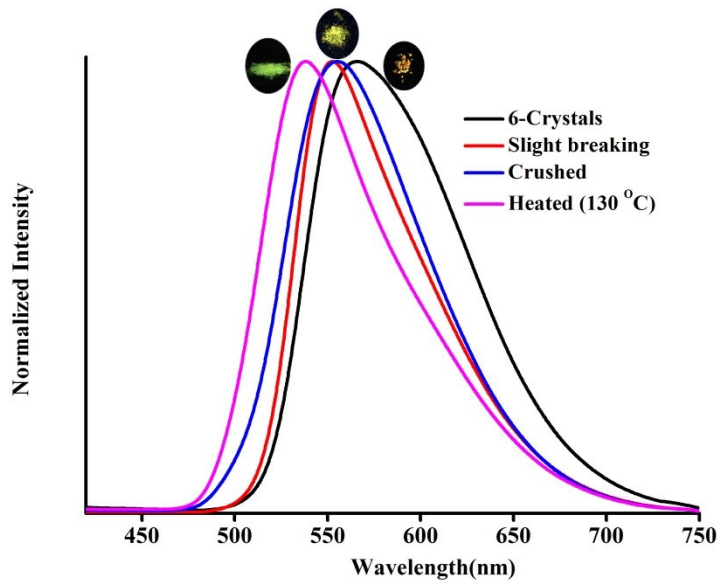


Fig. S38. MFC of **6**.

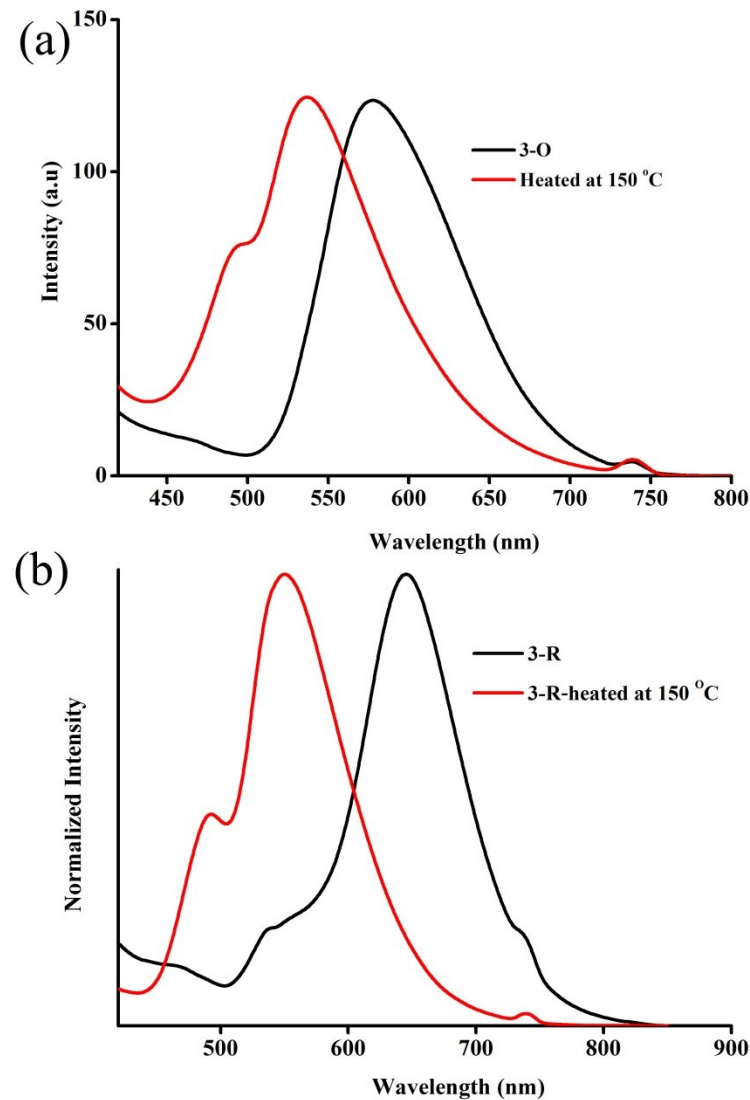


Fig. S39. Change of fluorescence upon heating the crystals of (a) **3-O** and (b) **3-R**.

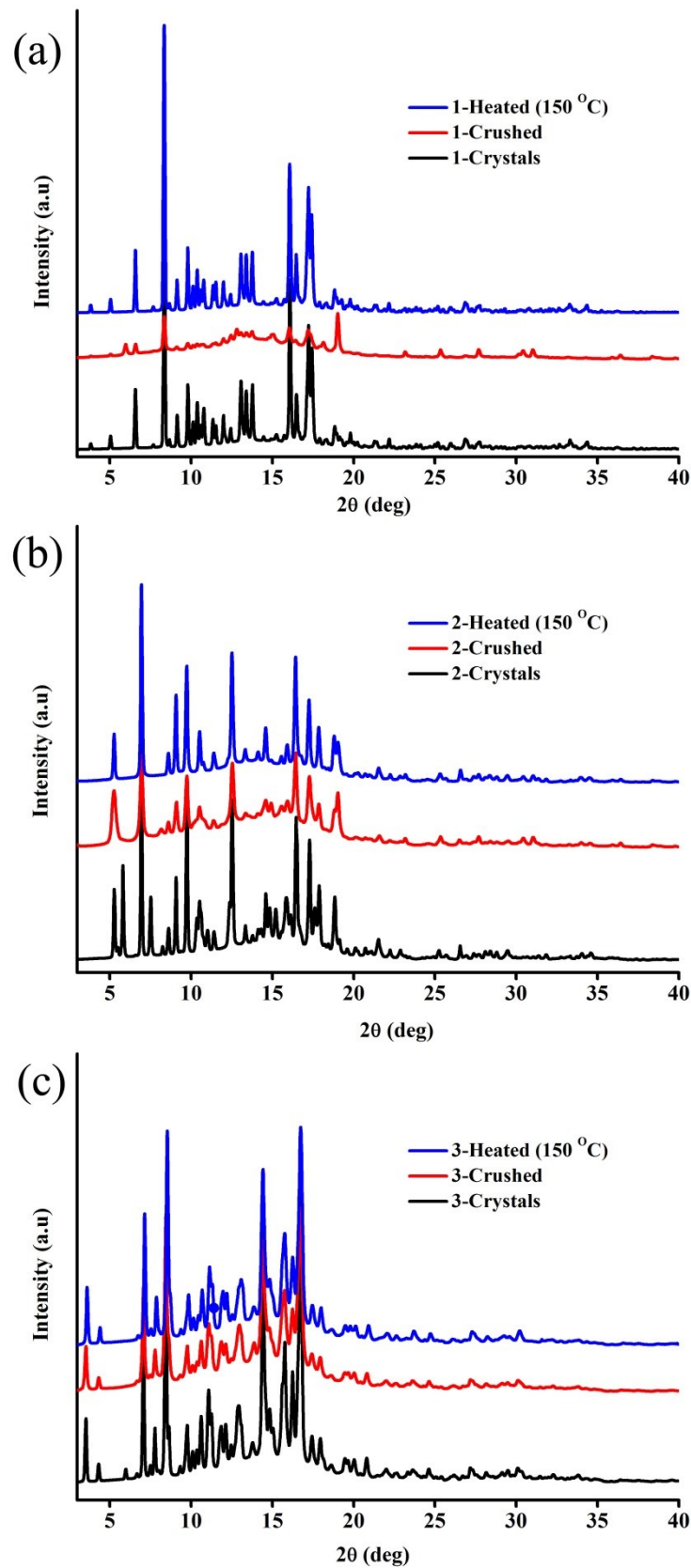


Fig. S40. PXRD patterns of (a) **1**, (b) **2** and (c) **3**.

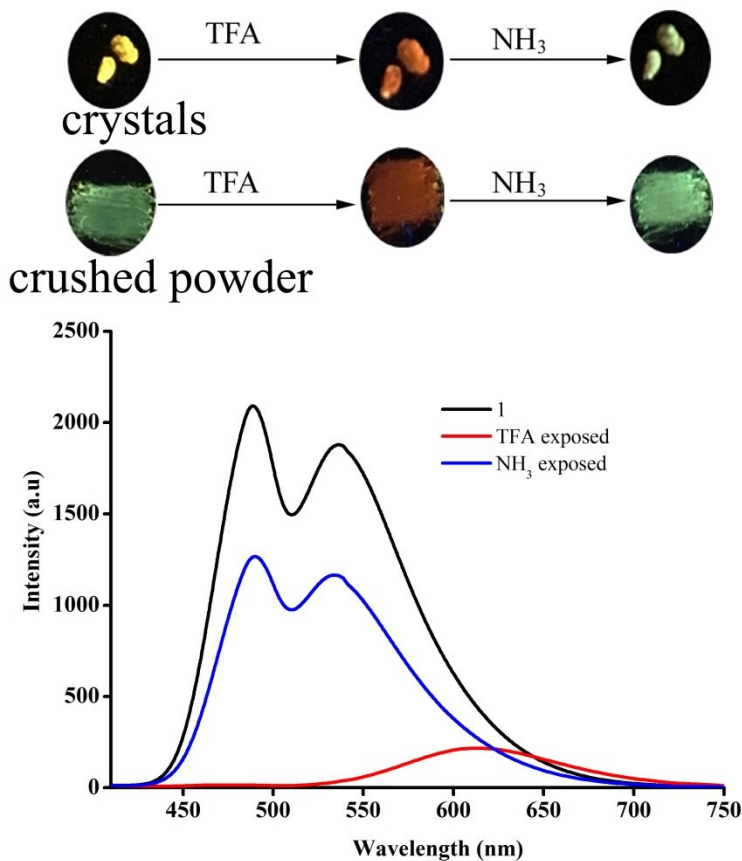


Fig. S41. Halochromic reversible fluorescence switching of **1**.

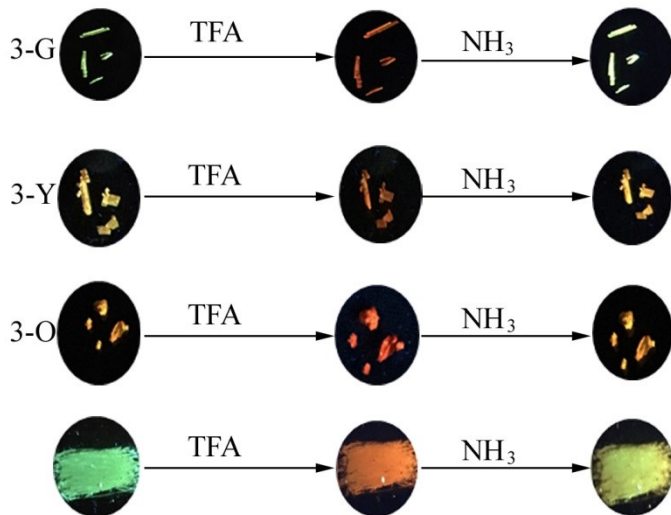


Fig. S42. Halochromic reversible fluorescence switching of **3**.

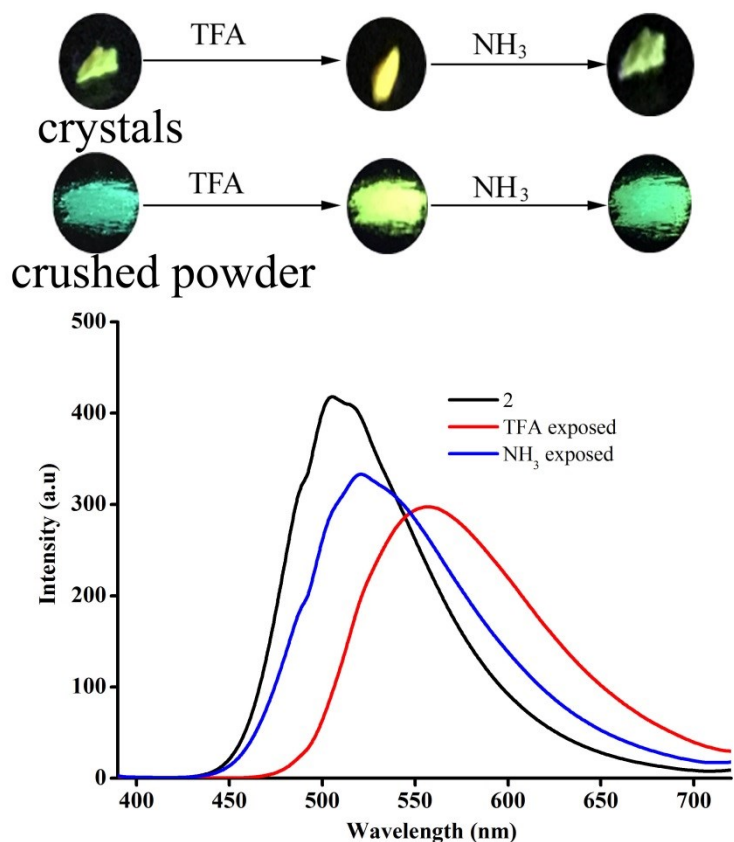


Fig. S43. Halochromic reversible fluorescence switching of **2**.

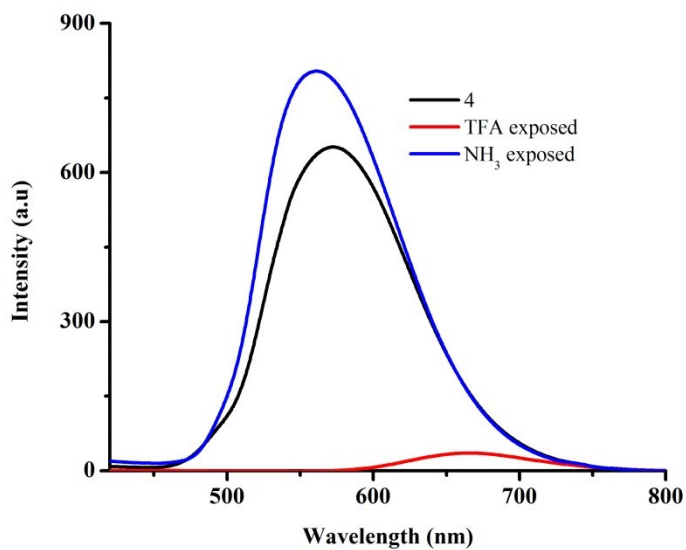


Fig. S44. Halochromic reversible fluorescence switching of **4**.

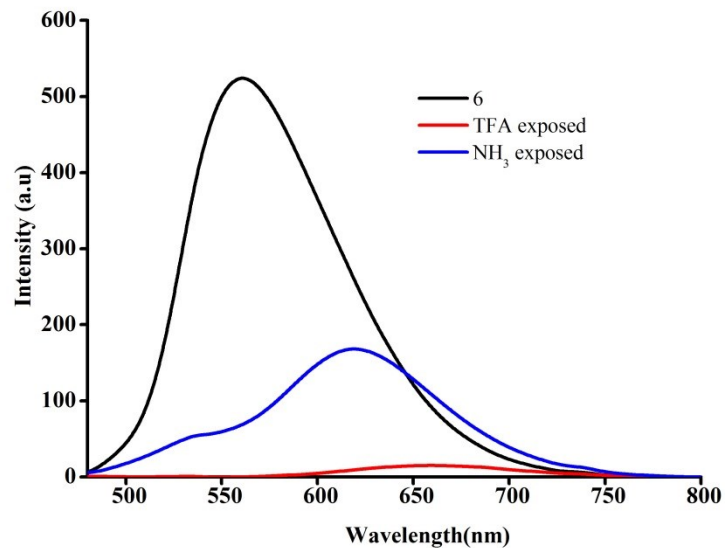


Fig. S45. Halochromic reversible fluorescence switching of **6**.

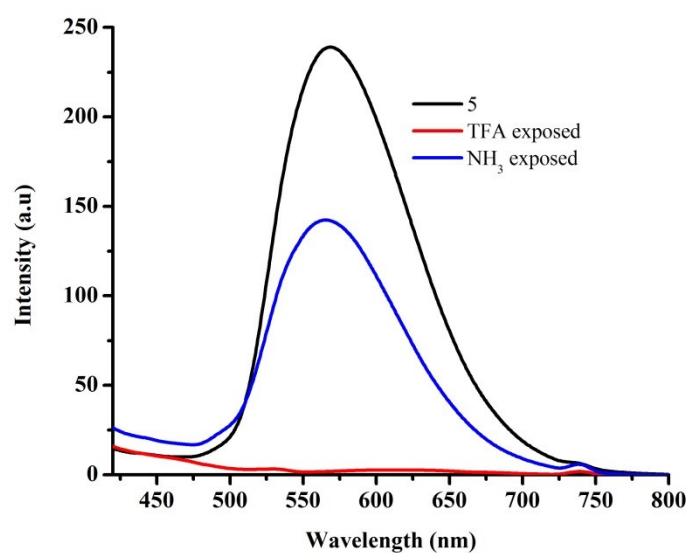


Fig. S46. Halochromic reversible fluorescence switching of **5**.

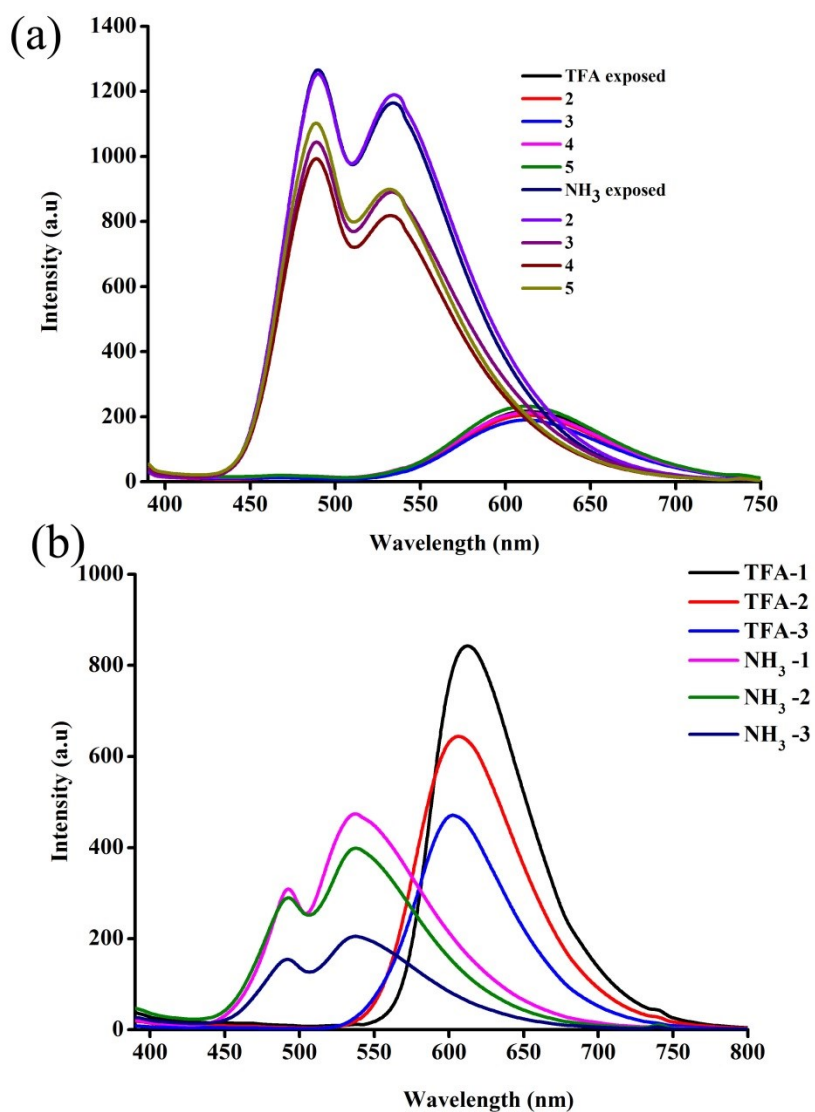


Fig. S47. Halochromic reversible fluorescence switching cycle of (a) **3** and (b) **6**.

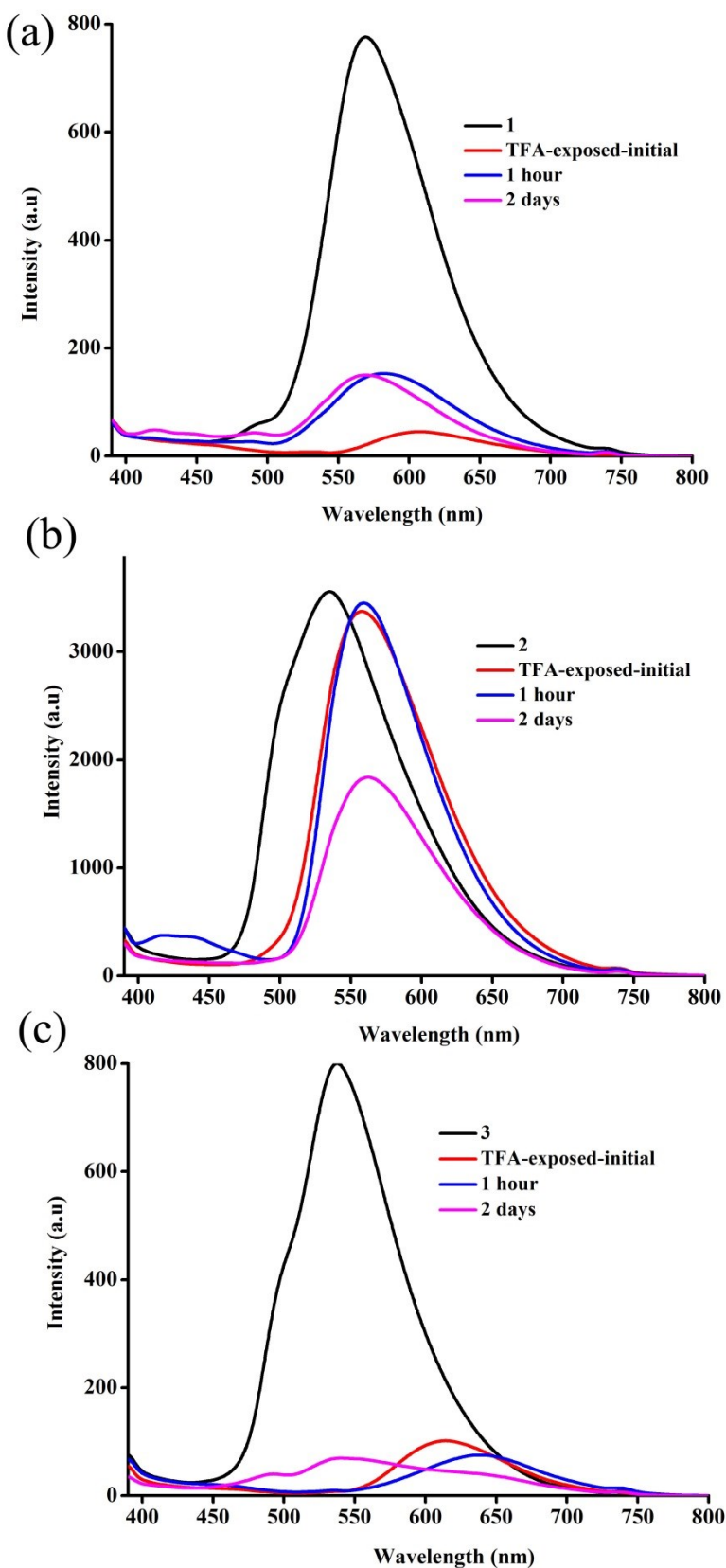


Fig. S48. Halochromic self-reversible fluorescence switching of (a) **1**, (b) **2** and (b) **3**.

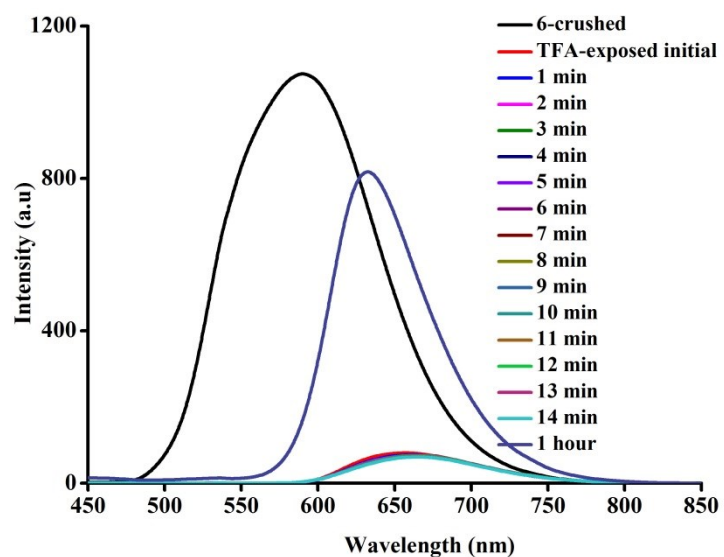


Fig. S49. Halochromic self-reversible fluorescence switching of **6**.

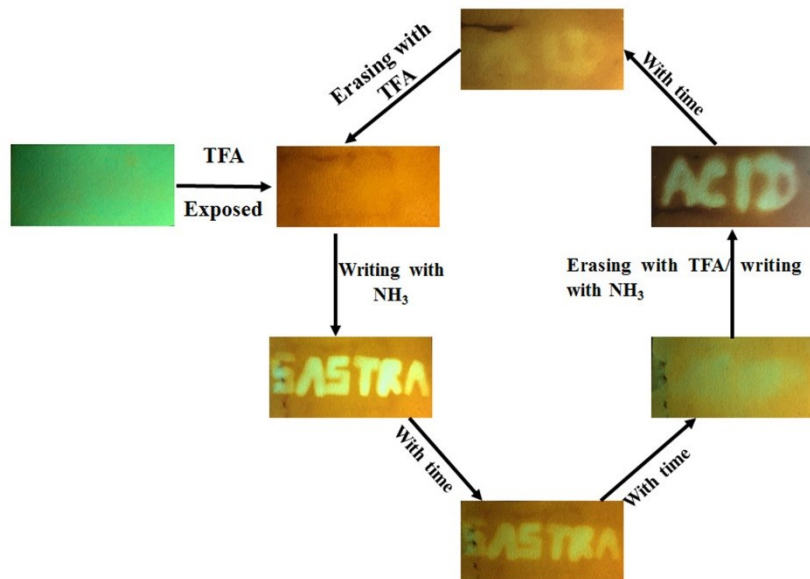


Fig. S50. Fabricating re-writable fluorescent platform using **3-PMMA** on filter paper.



Fig. S51. Fabricating re-writable fluorescent platform using **3-PMMA** on glass plate.

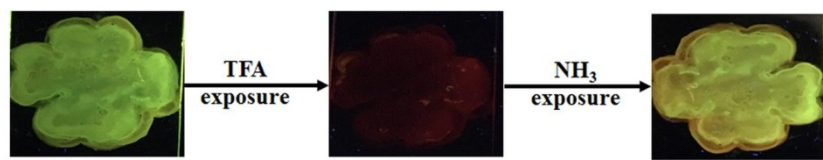


Fig. S52. Fabricating re-writable fluorescent platform using **6-PMMA** on glass plate.

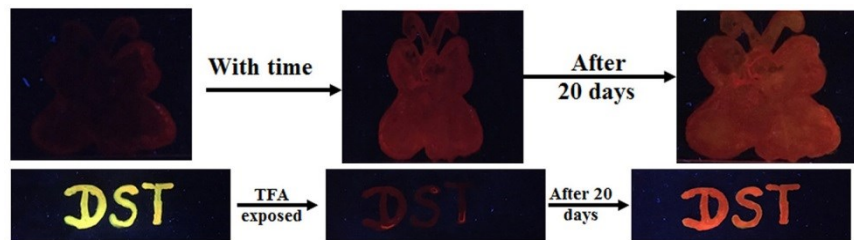


Fig. S53. Change of fluorescence intensity of **6-PMMA** on a glass plate.

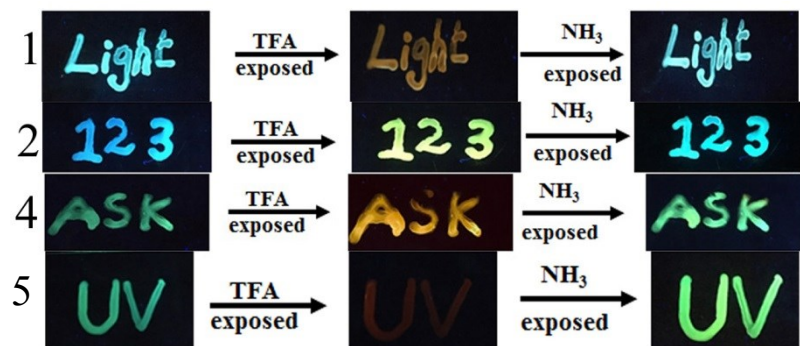


Fig. S54. Halochromic reversible fluorescence switching of **1-PMMA**, **2-PMMA**, **4-PMMA** and **5-PMMA** on a glass plate.